Expanded Shale, Clay and Slate Institute
Rotary Kiln Structural Lightweight Aggregate

SERVICE LIFE PREDICTION OF STRUCTURAL LIGHTWEIGHT CONCRETE USING TRANSPORT PROPERTIES

ESCSI Report 4363
October 2020

Edited by

Dr. Fariborz M. Tehrani, PhD, PE, ENV SP, PMP, SAP, F.ASCE

for

Expanded Shale, Clay and Slate Institute

Suggested Citation: Tehrani, F. M. "Service life prediction of structural lightweight concrete using transport properties." ESCSI Report 4363. Chicago: Illinois: Expanded Shale, Clay and Slate Institute, 2020. www.escsi.org

Table of Contents

Table of Figures

Table of Tables

Acknowledgements

This document reflects on the laboratory report by the Tourney Consulting Group, project number 16059, funded by the ESCSI and reviewed by Dr. Reid Castrodale and Dr. Matthew D. D'Ambrosia, and comments by Mr. Jeff Speck, ESCSI Chair, Mr. Kenneth Harmon, Structural Committee Chair, and other members of the ESCSI Structural Committee. Participating expanded shale, clay and slate producers in alphabetical order include Arcosa Lightweight, Carolina Stalite, DiGeronimo, Norlite, and Utelite.

Abstract

This report examines the effects of coarse and fine expanded shale, clay and slate (ESCS) aggregates on the transport properties of concrete. The transport properties are parameters in several service life analysis and simulation models, including STADUIM® and Life 365™ per *fib* Bulletin 34. Existing literature indicates the benefits of lightweight aggregate for enhancement of durability and service life of concrete infrastructure. This report demonstrates the quantitative assessment of such benefits on the transport properties of selected mixture proportioning designs using expanded shale, clay and slate aggregate. The methodology incorporates a simulation of the performance of a bridge deck in the Detroit area with the transport properties determined for use in Life 365™ or STADIUM®. The STADIUM® results showed that that the time to corrosion will be increased for lightweight mixtures compared to the control mixture with normal weight aggregates by approximately 22%. The replacement of normalweight sand with lightweight fines resulted in approximately a 34% to 88% increase in the time to corrosion. The Life 365™ analysis showed equivalent performance between lightweight coarse aggregate mixtures and the control mixture. As with STADIUM®, lightweight fines showed up to a three times improvement when replacing normalweight fines. Further, the internal curing mixture with a small quantity of lightweight fines improved time to restrained shrinkage cracking, increased strength, and extended the service life in comparison with the control concrete in both STADIUM® and Life 365™. Expanding the prediction model to various climate zones per FHWA verified the effectiveness of LWA in all zones and with the highest influence on the service life in dry and wet zones. Moreover, a comparison between different applications of structural lightweight concrete indicated the need for FLWA to enhance the service life of concrete in severe conditions such as marine tidal zones.

Introduction

Transport properties of concrete have been subject to extensive research as indicators of the durability of concrete and modeling parameters for predicting the service life of concrete [1-6]. Existing research suggests that application of lightweight aggregate enhances these properties in structural lightweight concrete [7-14]. Further, the internal curing using fine lightweight aggregate enhances the durability of normalweight concrete [15-21]. There are numerous models using transport properties to predict the service life of the concrete [22-25], including Life 365™ [26-29] and STADIUM® [30-45]. This study utilizes laboratory data to objectively assess the benefits of lightweight aggregate using these models.

1. Experimental Program

The experimental investigation considered fourteen mixtures with ten different sources of coarse and fine lightweight (LW) aggregate, in addition to the control mixture (C) with normalweight (NW) aggregate.

Lightweight mixtures included three containing both LW coarse aggregate (LWCA) and normalweight coarse aggregate (NWCA) with normalweight fine aggregate (NWFA), designated LW1; seven containing only LWCA and NWFA, designated LW2; one containing only LWCA and LWFA, designated ALW (all lightweight); one containing only NWCA and LWFA, designated LWF; and one containing NWCA and NWFA with a fraction of the NWFA replaced with LWFA, designated IC (Internally Cured). The reason for including NWCA in the mixtures designated LW1 was to keep the plastic densities and the coarse aggregate to fine aggregate ratios of the LW1 and LW2 mixtures relatively constant, with a target density of 120 pcf. Table 1 shows the designations used for various mixtures. Sources of lightweight aggregate included expanded shale, clay and slate (ESCS) [46]. Each mixture in LW1 and LW2 series had a different source of LWCA. The source of LWFA was the same for ALW, LWF, and IC mixtures. Further, all mixtures used the same sources of NWCA and NWFA, where applicable. Mixtures utilized Portland cement [47] only and did not use supplementary cementitious materials (SCMs) or corrosion inhibitors that would interfere with the service life of concrete, hence, results are indicators of the performance effects of LW only. However, mixtures utilized water reducing and air-entrainment admixtures per standard practice recommendations [48-49].

TABLE 1 MIXTURE DESIGNATIONS

Mixture Description	Designation
Control mixture with NW coarse and fine aggregates	C
Internally cured mixture with NW coarse and fine aggregates, plus LW fines	IC
Average for LW coarse aggregate with some NW coarse and all NW fine aggregates	LW1
Average for all LW coarse aggregate and NW fine aggregate	LW2
Reverse mixture with NW coarse aggregate and LW fine aggregate	LWF
LW coarse and fine aggregates without any NW aggregate	ALW

Table 2 provides a summary of the average volumetric fraction of lightweight aggregate contents in each mixture as a matrix, emphasizing the referenced contents as two independent variables.

TABLE 2 MIXTURE LIGHTWEIGHT AGGREGATE CONTENTS MATRIX

Mixture Designation		**Average Lightweight Coarse (Vol. %)**			
		0	30	39	37
Average Lightweight Fine (Vol. %)	0	C	LW1	LW2	
	10	IC			
	28	LWF			
	30				ALW

Table 3 shows the testing conducted for the fourteen mixtures including the control mixture (C). Restrained shrinkage testing was only conducted on the C and IC mixtures. The results include average values for each test, aggregated for all sources of lightweight aggregates. All tests follow the specified and other standard procedures by ASTM, ACI, and NT, including slump (ASTM C143), plastic air content (ASTM C231), hardened air content (ASTM C457) setting time (ASTM C403), temperature (ASTM C1064), compressive Strength (ASTM C39), Moisture content (ASTM C566), laboratory trial batching (ASTM C192 and ASTM C511), proportioning (ACI 211), internal curing (ASTM C1761), and transport properties (ASTM C1760, ASTM C1202, NT Build 492, ASTM C1556, ASTM C1585), and restrained shrinkage (ASTM 1581) [50-66].

Figure 1 and Figure 2 illustrate the average values for the equilibrium specific gravity (SG) and the 28-day compressive strength (normalized to the control mixture) of each mixture designation, respectively. The specific gravities of the mixtures in these figures reflect the plastic and equilibrium densities. The specific gravity of fine aggregate is higher than that of coarse aggregate from the same source, and this is reflected in the SG and density

of the mixtures. The average oven dry specific gravity of these mixtures is nearly equal to 1.79, hence, indicating that the equilibrium moisture is not a major factor in the observed difference. The influence of lightweight aggregate content on the average compressive strength is clear, as the substitution of NW aggregate with LW, either LWCA or LWFA, has increased the reported strength.

TABLE 3 TEST PROGRAM PER MIXTURE DESIGN

Tests	Per Mix	Notes
Plastic Properties (slump, air setting time)	1	For each Mix
Compressive Strength	3	1, 28, 90 days
STADIUM Transp. (IDC, MTC, ASTM 642 porosity)	2	28 and 90 days
ASTM C1760 Bulk Conductivity	2	28, 90 days
NT Build 492 Non-Steady State Diffusion Coefficient	1	28 days
ASTM C1556 Bulk Diffusion	1	28 days
ASTM C1585 Capillary Absorption	1	28 and 90 days LWA
ASTM C1581 Restrained Shrinkage	1	Only for IC mix and Control

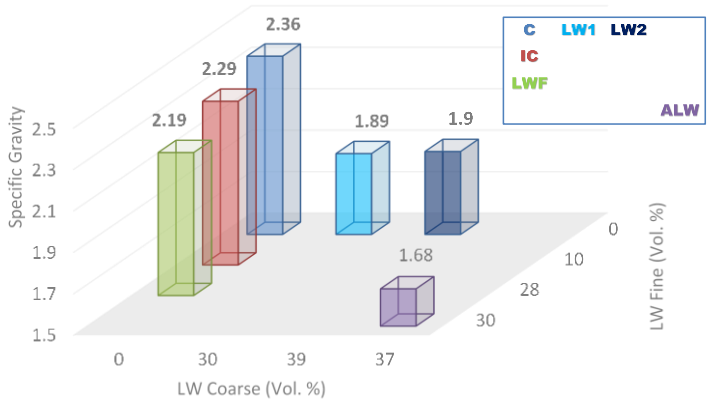

FIGURE 1 MIXTURE SPECIFIC GRAVITY AVERAGE VALUES

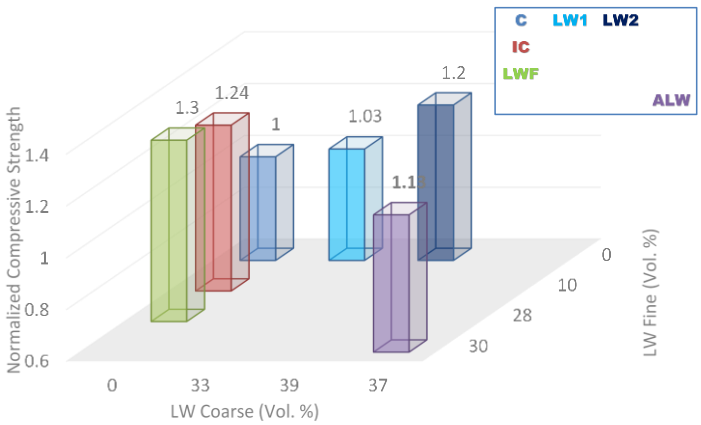

FIGURE 2 MIXTURE 28-DAY COMPRESSIVE STRENGTH AVERAGE VALUES

Description of Transport Tests

STADIUM® modeling software utilizes two transport properties. The first is the ionic diffusion coefficient (IDC), which represents the movement of chloride and other ions through the capillaries. The second is the moisture transfer coefficient (MTC), which represents chloride ingress when the concrete is not 100% saturated. The latter is unique to STADIUM® and highly relevant when conducting service life analysis. Note that the STADIUM® modeling program accounts for the movements of multiple species in the concrete as well as for chemical reactions and binding reactions. This allows for a prediction of the chloride-to-hydroxide levels, which is important for comparing mixtures with supplementary cementitious materials (SCMs) [45].

The ASTM C1760 Bulk Conductivity test is directly related to the ASTM C1202 Rapid Chloride Permeability, but it is non-destructive, as it is conducted for a short time and does not subject the specimens to heating. The bulk conductivity is used to monitor the change in permeability over time, as it is directly related to the diffusion coefficients [61-62].

The NT Build 492 provides a relatively rapid (1 to 2 days) indication of chloride ingress. It adjusts for an increase in conductivity that is not related to chloride ingress. The results are used in the *fib* service-life analysis [63, 24].

The ASTM C1556 Bulk Diffusion is used to calculate the apparent diffusion coefficient for the chloride ingress and can be used in Life 365™ or the *fib* service-life analysis [64, 28, 24].

ASTM C1585 Capillary Absorption is used to predict the surface concentration of chloride when the concrete is not water saturated. It can be used in Life 365 ™ and the *fib* service-life analysis. This is of primary use when there is wetting and drying of the surface. In Life 365™, the time to reaching the maximum surface concentration is decreased or increased compared to a control concrete, based upon the ratio of the absorption values [65, 28, 24].

Concrete Plastic and Mechanical Properties

Table 4 shows batching data and the concrete proportions, plastic, and mechanical properties for all the mixtures, including average results and standard deviations for LW1 and LW2. The LW1 represents an average of the three lightweight coarse aggregate concrete mixtures that required NWCA to achieve the target plastic density while maintaining the coarse to fine aggregate ratio. The LW2 is the average for the seven lightweight coarse aggregate concrete mixtures made without normalweight coarse aggregate. The data analysis provides insight on variation of properties for different sources of LWCA, as well as trends of changes as a function of substituting NWCA and NWFA with LWCA and LWFA, respectively. Figure 3 shows the drying of the 6 x 12-in. cylinders in the controlled relative humidity and temperature (RH/T) room according to ASTM C567 [69], as well as other drying specimens.

FIGURE 3 DRYING SPECIMENS. MTC SPECIMENS (LEFT), ASTM C1585 (CENTER) AND ASTM C567 (RIGHT)

Mix Preparation Procedures

The saturation of LWCA began with submerging them in a sealed pail and adding water for one day. The LWCA remained submerged in water for a minimum of 7 days, and then, drained in the fog room to lose the excess water. The procedure for LWFA included oven drying, adding 20% water in the concrete mixer as the average absorption rate, and placement in sealed pails to keep the moisture until mixing. The absorption rate for a sample of LWFA was between 18.78 and 22.2% per ASTM C642 and NY 703-19E method [67-68].

Figure 4 exhibits the volumetric content of materials in each mixture. These data indicate the small fluctuations in the volumetric content of lightweight coarse aggregate in mixture series LW1 and LW2 with a nearly identical coefficient of variation (CV) of 10%. The LW1 mixture contained the same fraction of normalweight fine aggregate. However, this value for LW2 is 18%. Similarly, the CV of the normalweight coarse aggregate in the LW1 mixture was 43%.

TABLE 4 CONCRETE MIXTURE PROPORTIONS, AND PLASTIC AND MECHANICAL PROPERTIES

Mixture Description	LW1 Mean	LW1 S.D.[3]	LW2 Mean	LW2 S.D.[3]	ALW	LWF	IC	C
Cement, Lafarge Alpena Type I (lb./yd^3)	658	0	658	0	658	658	658	658
Natural Fine Aggregate, Midway Pit, SSD[1] (lb./yd^3) , SG[2] 2.80	1341	16	1240	203	0	0	846	1294
Natural Coarse Aggregate, Bay Cedarville Pit Limestone #67, SSD[1] (lb./yd^3), SG[2] 2.65	317	125	0	0	0	1800	1800	1800
Lightweight Coarse Aggregate, SSD[1] (lb./yd^3) , SG[2] varies	671	149	1097	159	1115	0	0	0
Lightweight Fine Aggregate, SSD[1] (lb./yd^3) , SG[2] 1.79	0	0	0	0	917	833	304	0
Total Water (lb./yd^3)	248	3	243	1	243	243	243	243
Designed Air (%)	6.33	0.24	6.5	0.46	6	6	6	6
Designed Plastic Density (lb./ft^3)	119.9	0.7	119.9	2	108.7	130.9	142.6	148
Water/Cementitious Materials (w/cm) Ratio	0.38	0	0.37	0	0.37	0.37	0.37	0.37
Admixtures								
BASF Master Air AE100 (oz/cwt)	0.2	0	0.2	0	0.2	0.2	0.4	0.5
BASF Glenium 7500, HRWR (oz/cwt)	3.5	0.2	4.5	0.8	4.3	5.3	5	4.4
Physical Properties								
Slump (in.)	4.2	0.6	4.5	2	3	5	7.5	4
Measured Volumetric Air (%)	7.4	0.5	6.7	0.4	6.25	6	7	7.1
Water Saturated Bulk Density (lb./ft^3)	50.6	11.4	57.9	2.4	57.6	53.3	53.3	
Concrete Plastic Density (lb./ft^3)	120.7	1.8	122.2	1.9	109.8	133.3	141.6	146.2
Concrete Oven Dry Density (lb./ft^3)	111.5	2	111.4	2.8	95.6	130.1	137.2	142.1
Concrete Equilibrium Air Density (lb./ft^3)	118	1.9	118.8	2.2	104.8	136.5	142.9	147.3
Days to Reach Equilibrium (avg. 2 per mixture)	93	13	116	28	140	84	84	56
Compressive Strength								
1-Day Strength, average of 3 tests (psi)	2870	210	3370	420	2700	3500	3570	3310
28-Day Strength, average of 3 tests (psi)	5650	280	6540	540	6160	7120	6760	5470
90-Day Strength, average of 3 tests (psi)	6260	410	7240	640	7140	8040	7743	5950

[1] Saturated Surface Dry
[2] Specific Gravity
[3] Standard Deviation

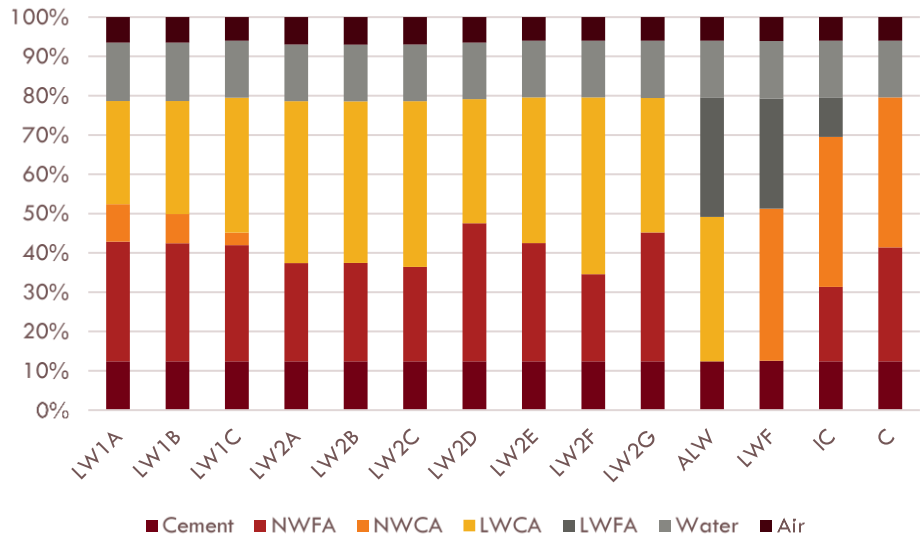

FIGURE 4 MIXTURE VOLUMETRIC PROPORTIONS

Concrete Testing

Table 4 shows that the densities of the air-dried concrete mixtures were, as expected, higher than the oven-dry specimens. The lightweight mixtures show a larger difference than the C and IC mixtures, indicating that the air-dried LW aggregates are retaining moisture. Figure 5 presents variations of specific gravity as a function of coarse and fine lightweight aggregate content in a three-dimensional format, confirming the previous observations and emphasizing the relative fluctuation of these values for LW1 and LW2 samples. Although there is no reliable dependency between the LWCA content and the specific gravity of LW1 and LW2 samples, a general weak form of dependency is apparent for the average values of these mixtures. The expression for the presented linear model with 95% confidence includes -19±3.9% and -6.4±3.9% slopes for LWCA and LWFA, respectively.

Reported compressive strengths in Table 4 indicate an increase for mixtures containing lightweight aggregate, including the IC, in comparison with the control mixture C. The increase in strength could be an indication of better bond between aggregate and cementitious matrix, as well as enhanced hydration in presence of LW aggregate. Figure 6 examines the density-strength values of mixtures and the proximity of LW1 and LW2 results. It is evident that LW1 mixtures had lower 28-day compressive strength values than LW2 mixtures with similar specific gravity values. Figure 7 supplements the prior figure and communicates the weak relationship between the specific gravity and the lightweight aggregate content, suggesting the independency of these values.

Figure 8 provides similar results for the 28-day compressive strength values. Hence, there is no established bias in respect to the sources of LWCA in LW1 and LW2 mixtures, influencing specific gravity or compressive strength values. Further, the LWFA content has no meaningful influence on the specific gravity on mixture series LWF-IC-C, but it increases the compressive strength, even though there are not enough samples on the latter observation to establish a meaningful confidence level.

Figure 9 presents variations of compressive strength as a function of coarse and fine lightweight aggregate content in a three-dimensional space. The compressive strength represents the normalized 28-day strength as a ratio to the control mixture. It is evident from the data analysis associated with this figure that the proposed polynomial relationship with R-square of 38% is not a fit for the trends of the strength. The low fidelity of the fit hints toward the independency of strength from the LW content in mixtures, that is, there is no meaningful bias in the strength of mixtures in respect their LW aggregate content. Regardless, the loose fit in the strength-LWFA and strength-LWCA planes warrants the opportunity to establish a relationship for the optimized LW contents using a larger population of samples. The current data suggests such optimum value at 22% LWCA and 17% LWFA contents, albeit with a large margin of error.

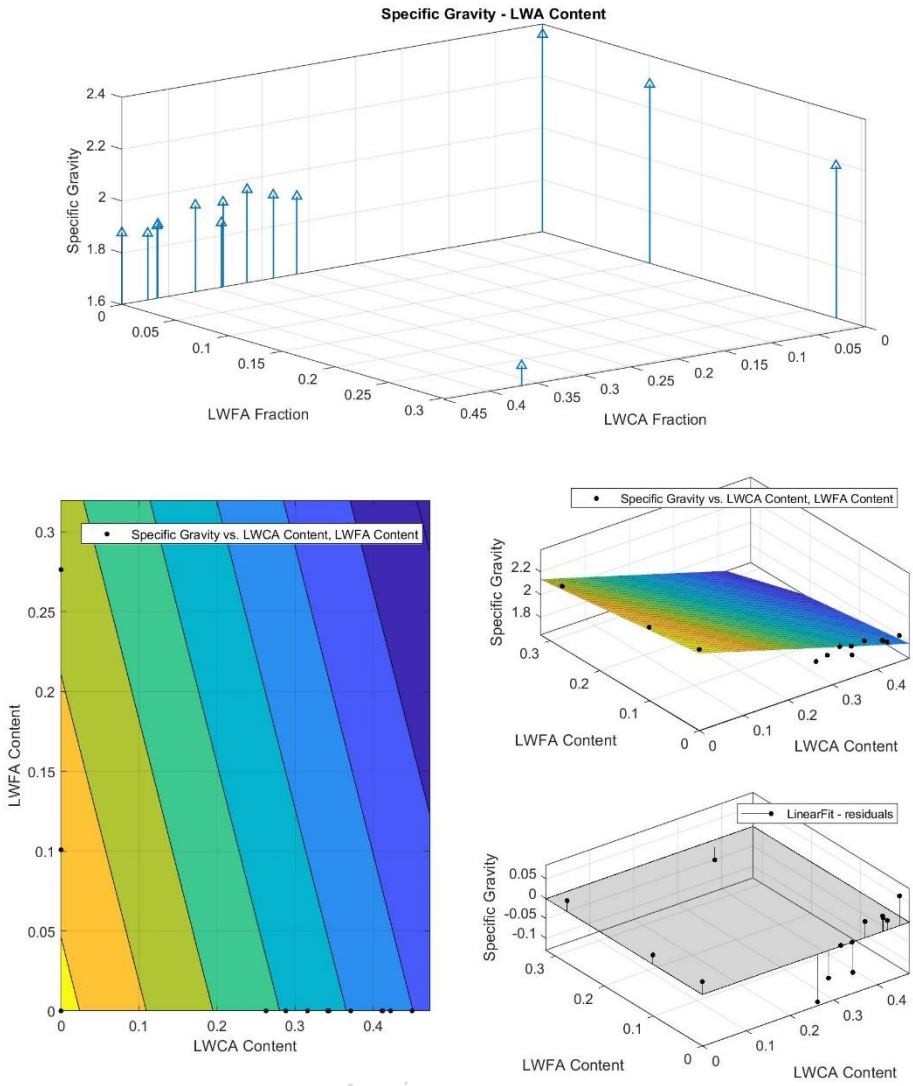

FIGURE 5 MODELING SPECIFIC GRAVITY (TOP), FITTING PLANE (MIDDLE), CONTOURS (BOTTOM LEFT), AND ERROR (BOTTOM RIGHT)

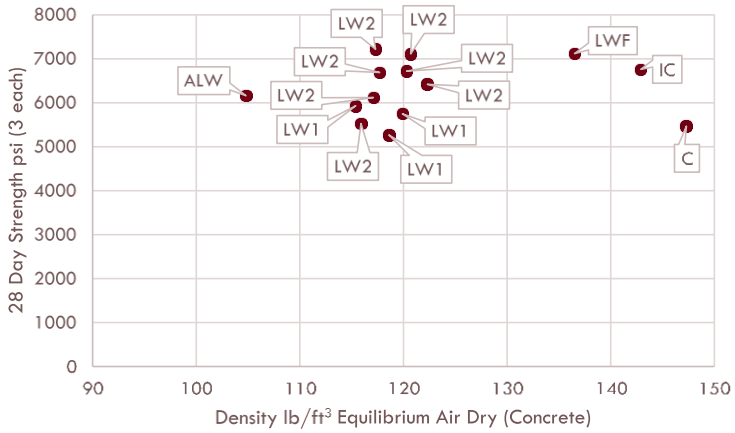

FIGURE 6 DENSITY-STRENGTH-MIX RELATIONSHIPS

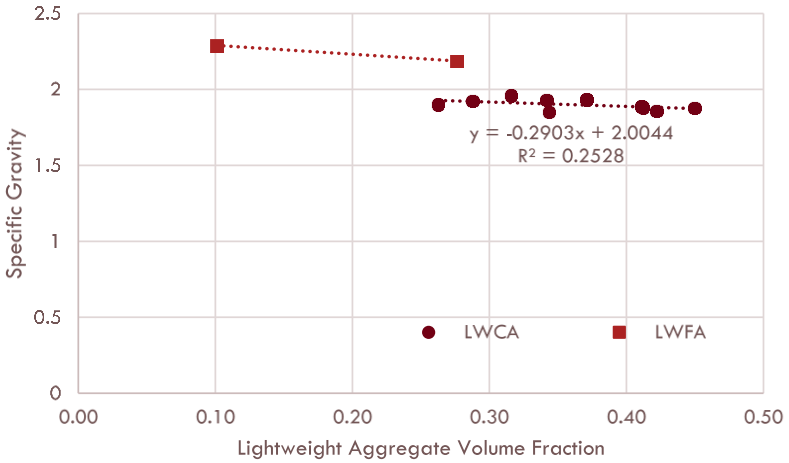

FIGURE 7 SPECIFIC GRAVITY - LW CONTENT RELATIONSHIPS

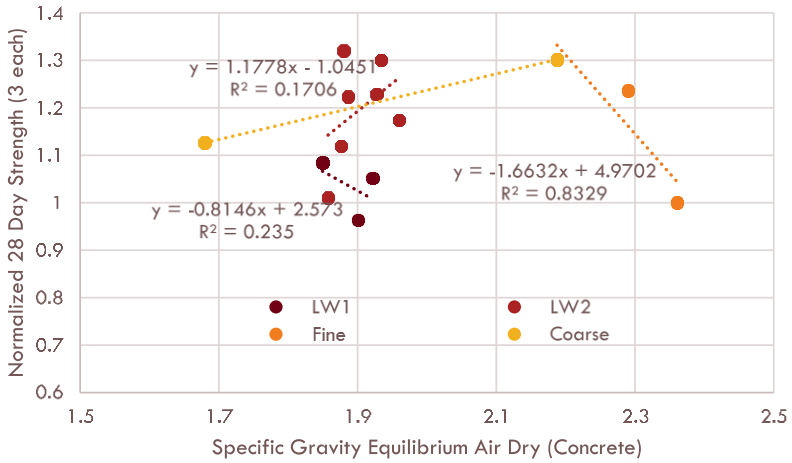

FIGURE 8 DENSITY-STRENGTH-LW CONTENT RELATIONSHIPS

Figure 10 traces the strength gain for each mixture over the first 90 days. This figure presents that reported compressive strength values fall within the mean plus-minus three standard deviation range at day 1 but fit a narrower range of the mean plus-minus two standard deviation at day 28 and 90. Figure 11 provides a comparison between these distributions using normalized parameters. This figure shows that distributions at 1-day and 28-day have positive (0.6) and negative (-0.1) skews, respectively. The 90-day values also indicate a negative skew (-0.3). Distributions show kurtosis values of 0.6, -1.3, and -1 for 1-, 28-, and 90-day, respectively.

Table 5 contains porosity results of LW aggregate and concrete mixtures per ASTM C642 [67]. The porosity of the LWFA was assumed the same as the LWCA from the same source. The porosity of the concrete was then adjusted for the volume of porosity in the LW aggregates in a unit volume. The volume of permeable voids in the aggregate is typically less than the aggregate porosity, hence an adjustment was applied using the following expression for each individual mixture, shown as average values for LW1 and LW2 in Table 5.

$$\varphi' = \varphi - (V_v V_{av} V_s)$$

where φ' is the corrected porosity, φ is the measured porosity per ASTM C642, V_v is the volume of voids in the LW aggregate, V_{av} is the volume of accessible voids, and V_s is the total solid volume of coarse and fine LW aggregates.

The correction for control mixture is negligible due to low porosity of NW aggregate. After correcting for the voids in the aggregate, the porosity of LW mixtures was similar or lower than the porosity of the control mixture (Figure 12).

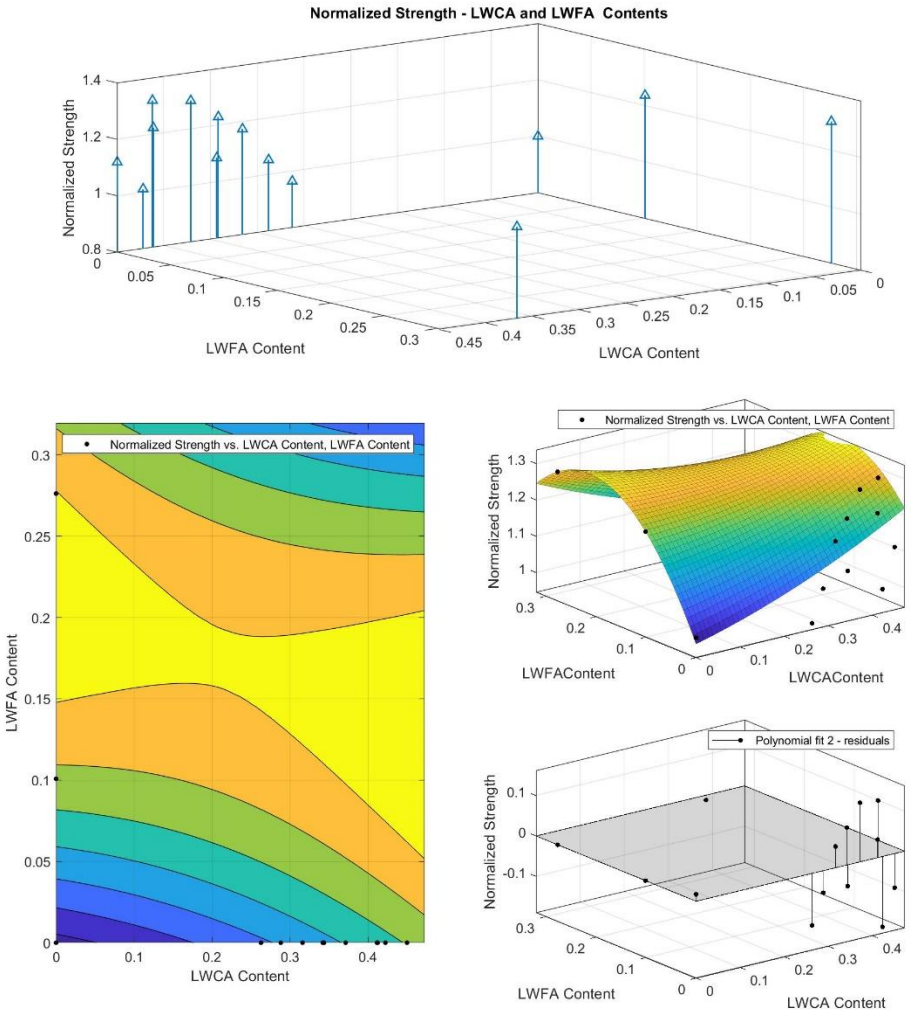

FIGURE 9 MODELING 28-DAY STRENGTH, PSI (TOP), FITTING PLANE (MIDDLE), CONTOURS (BOTTOM LEFT), AND ERROR (BOTTOM RIGHT)

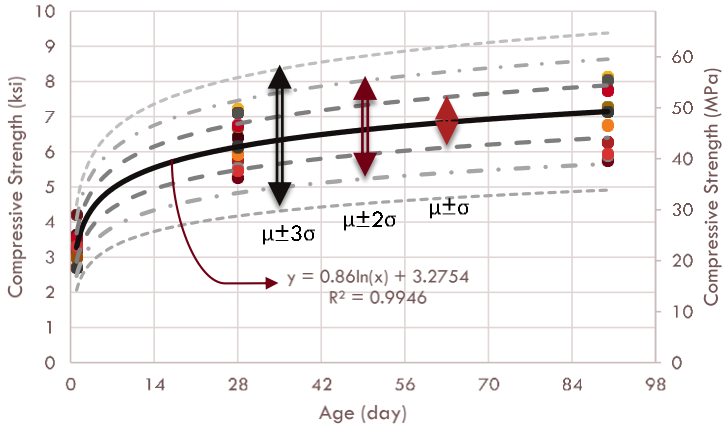

FIGURE 10 CHANGES IN THE COMPRESSIVE STRENGTH

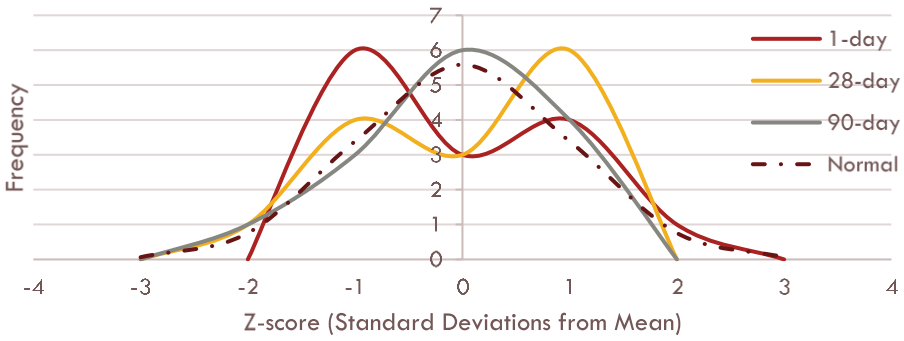

FIGURE 11 NORMALIZED COMPRESSIVE STRENGTH DISTRIBUTION VERSUS NORMAL DISTRIBUTION

TABLE 5 CORRECTED POROSITY DATA C642 POROSITY DATA

Property	LW1 Mean	LW1 Std. Dev.	LW2 Mean	LW2 Std. Dev.
Volume of Permeable Voids (%)	15.4	0.9	17.0	2.7
Voids in LWA (%)	33.8	1.5	32.2	9.3
Accessible voids in LWA (%)	48.3	2.4	54.0	8.6
Solid Volume of LWCA (ft^3/yd^3)	16.5	0.7	14.7	4.5
Corrected Volume of Permeable Voids (%)	10.57	1.3	10.65	0.9

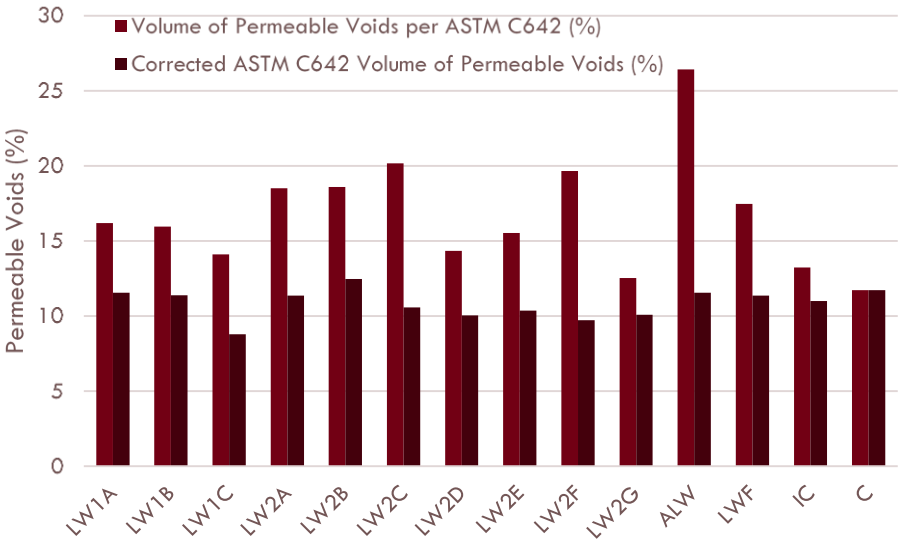

FIGURE 12 MEASURED AND CORRECTED POROSITY OF MIXTURES

Presented results contain conductivity and resistivity properties, along with calculated normalized ratios. The bulk conductivity is related to the ASTM C1202 [62] Coulomb values as it represents the initial reading in that test. If there is no increase in the temperature of the specimens, then the bulk conductivity would be related to the final Coulomb value, which is typical for low permeability concretes with SCMs. Experimental results have predicted ASTM C1202

values assuming no heating. These values are more closely related to diffusion values. The surface resistivity at 28 days was converted using the relationship developed by Weiss et al at 28 days [70-75].

As shown in Figure 13, only the IC concrete has a lower predicted ASTM C1202 Coulomb value than the C concrete at both 28 and 90 days. The LWF concrete has a lower Coulomb value than the C concrete at 90 days. As will be seen, the higher Coulomb values for the lightweight mixes are not associated with faster chloride ingress, but a reflection on the higher ionic conductivity due to the water in the aggregates.

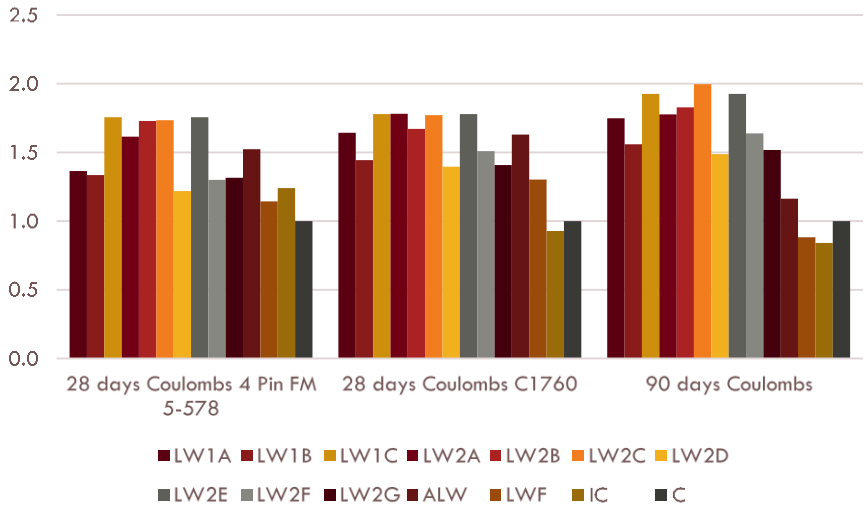

FIGURE 13 COMPARISON OF COULOMBS VALUES

Figure 14 and Figure 15 provide a comparison between conductivity values using bulk and surface methods at 28- and 90-day ages. These figures indicate that presence of LWCA has increased the conductivity by both means of measurements and at both reported ages. Substitution of NWFA with LWFA in LWF mixtures has increased conductivity at 28-day age but has decreased that value at 90-day age. The trend of conductivity for IC mixture is not consistent, as recorded surface measure is higher than bulk measure for the IC mixture in comparison to the C mixture. It is notable that these electrical measurements of conductivity (or resistivity) are affected by the internal water present in the LW aggregate as part of the pore transport fluid, even though this porosity is not interconnected with respect to true ion transport.

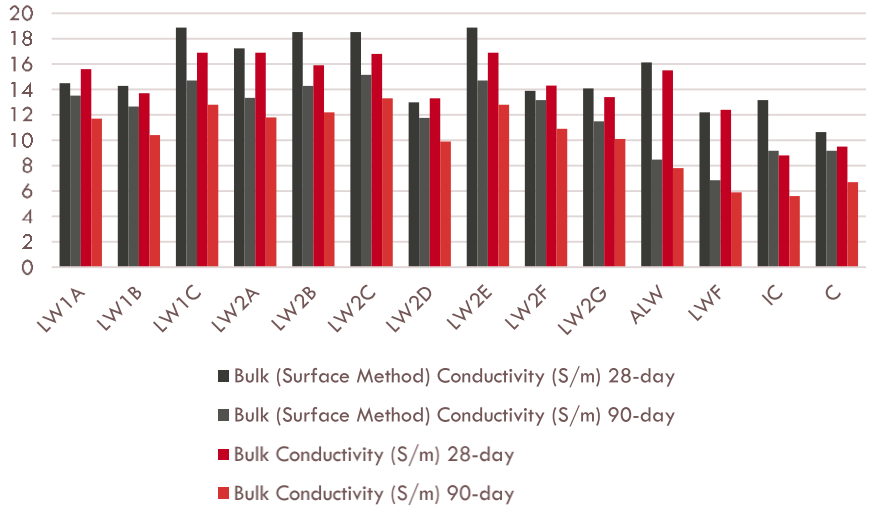

FIGURE 14 CONDUCTIVITY DATA

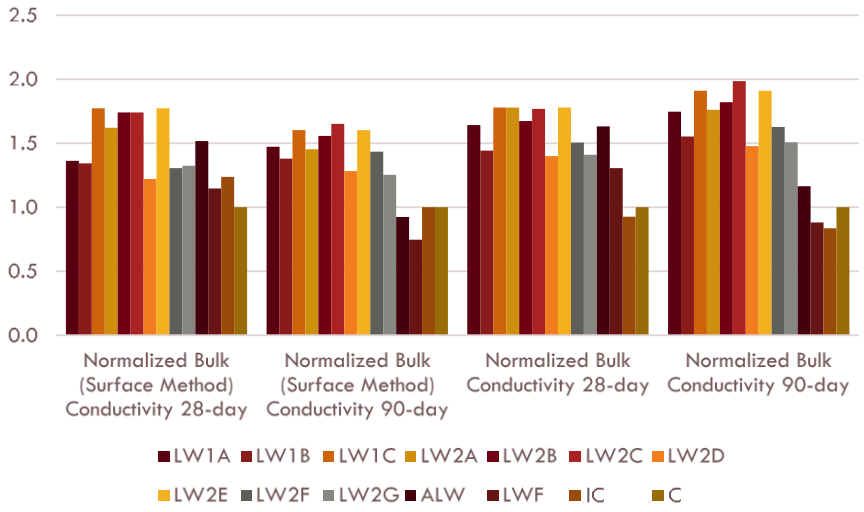

FIGURE 15 NORMALIZED CONDUCTIVITY DATA

Table 6 provides a summary of average values for LW1 and LW2 mixtures in comparison with other mixtures. Comparison of standard deviations indicates that the bulk surface measures converge to less scattered values as the concrete ages than the bulk measures. Further, the ratio between these measures show less scatter as the concrete ages, providing higher reliability for comparing these values. This comparison is essential for using conductivity values as main parameters in determining the service life of concrete and allows interpretations to place less emphasis on short-term (28-day) records rather than long-term (90-day) records.

TABLE 6 CALCULATED CONDUCTIVITY DATA

Transport Property	LW1 Mean	LW1 Std. Dev.	LW2 Mean	LW2 Std. Dev.	ALW	LWF	IC	C
28 d Bulk Resistivity (kΩ-cm) 4 Pin	6.4	0.8	6.3	0.9	6.2	8.2	7.6	9.4
28 days Coulombs 4 Pin FM 5-578	2883	372	2958	424	2957	2220	2408	1941
90 d Bulk Resistivity (kΩ-cm) 4 Pin	7.4	0.4	7.5	0.8	11.8	14.6	10.9	10.9
28 d Bulk Conductivity (mS/m) C1760	15.4	1.3	15.4	1.5	15.5	12.4	8.8	9.5
28 d Std Dev (mS/m) C1760	0.3	0.2	0.2	0.1	0.001	0.1	0.02	0.4
28 days Coulombs C1760	2799	237	2790	280	2814	2248	1601	1726
90 d Bulk Conductivity (mS/m)	11.6	1.0	11.6	1.2	7.8	5.9	5.6	6.7
90 d Std Dev (mS/m) C1760	0.2	0.2	0.2	0.1	0.019	0.009	0.015	0.3
90 days Coulombs	2114	181	2108	221	1410	1069	1020	1212
Bulk Surface Conductivity (S/m) 28-day	15.9	2.11	16.3	2.36	16.1	12.2	13.2	10.6
Bulk Surface Conductivity (S/m) 90-day	13.6	0.84	13.4	1.31	8.5	6.8	9.2	9.2
Bulk Conductivity (S/m) 28-day	15.4	1.31	15.4	1.53	15.5	12.4	8.8	9.5
Bulk Conductivity (S/m) 90-day	11.6	0.98	11.6	1.22	7.8	5.9	5.6	6.7

Figure 16 and Figure 17 confirm prior observations that the measured conductivities of LWCA mixtures were higher, while the LWFA mixture had lower conductivity and the IC mixture had little effect on the conductivity.

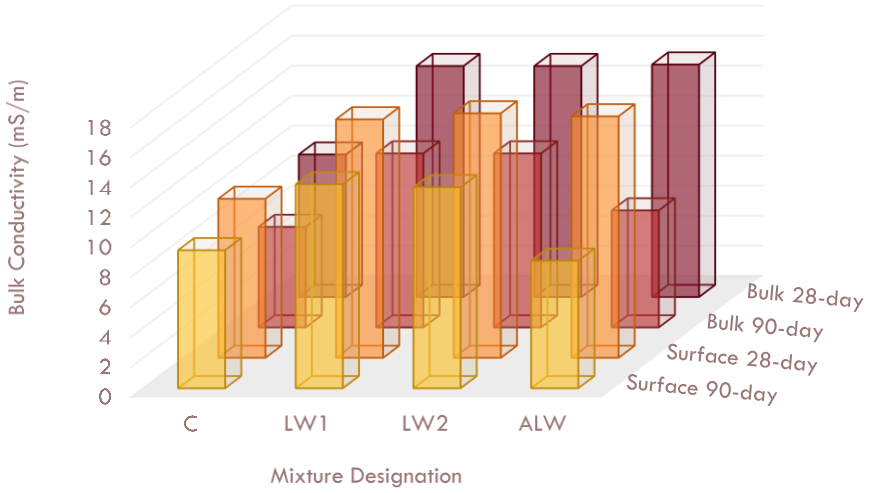

FIGURE 16 BULK CONDUCTIVITY FOR LWCA CONTENTS

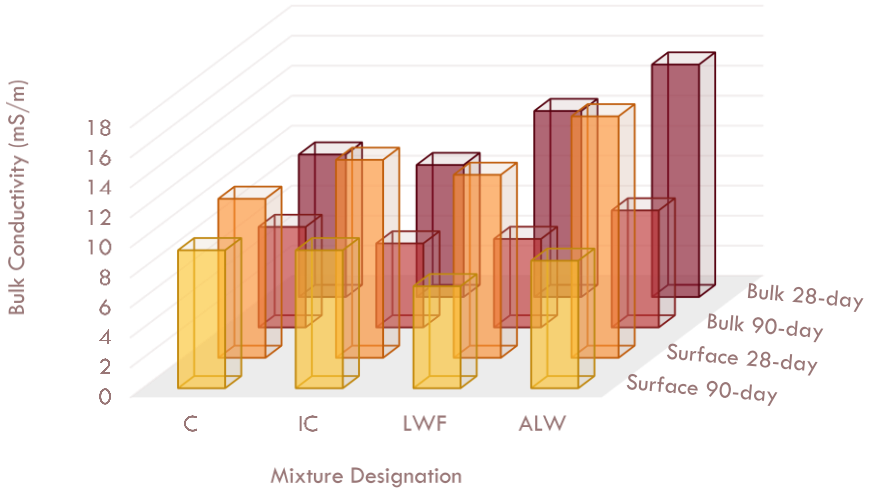

FIGURE 17 BULK CONDUCTIVITY FOR LWFA CONTENTS

Figure 18 shows variation of bulk conductivity at 90-day using surface method as a function of LWCA and LWFA contents. The R-square measure for the proposed fitting is 86.75%, indicating a low fidelity relationship. Comparing the LWCA and LWFA planes show that the higher influence of LWCA content on the conductivity than the LWFA content.

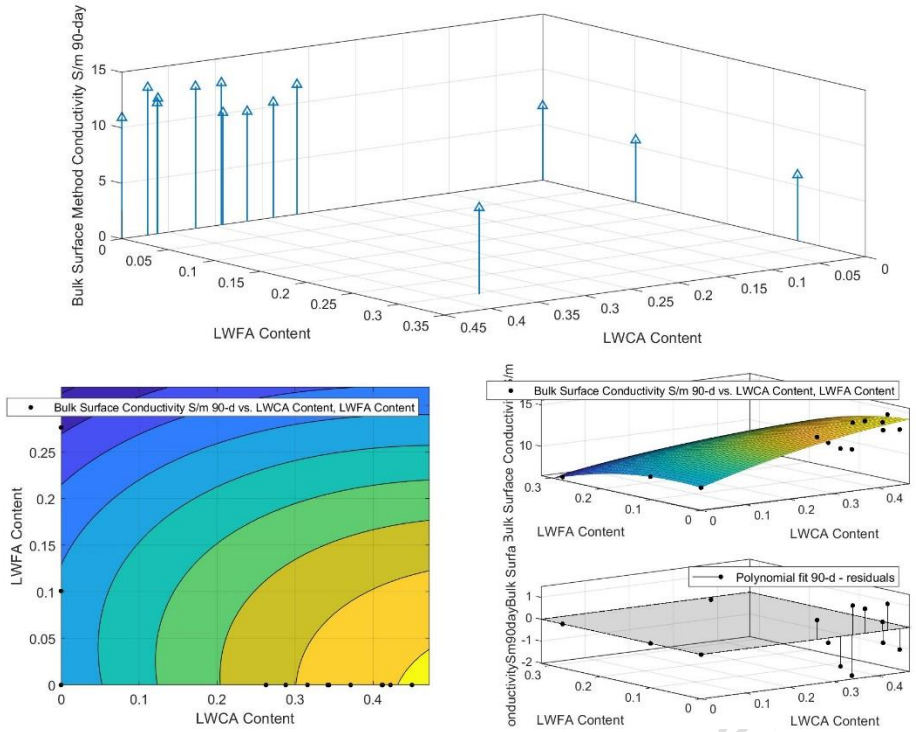

FIGURE 18 TRENDS OF BULK (SURFACE METHOD) CONDUCTIVITY AT 90-DAY (TOP), FITTING PLANE (MIDDLE), CONTOURS (BOTTOM LEFT), AND ERROR (BOTTOM RIGHT)

Figure 19 exhibits the relationship between the inverse of surface resistivity (surface conductivity) and the bulk conductivity, and their changes as concrete ages from 28- to 90-day. However, as one is measuring a surface effect and the other a bulk property, they will be different. Figure 20 indicates that the relationship, however, is steady for nearly all lightweight mixtures, with an exception of the IC, where the ratio between surface and bulk measures are higher than other mixtures. The surface resistivity can be correlated to the bulk conductivity at a given time. Figure 21indicates that presence of LWFA has more influence on the reduction of both measures of conductivity from 28- to 90-day ages than LWCA. The bulk conductivity is more closely related to the strength and diffusion values, which are bulk properties. The decrease of conductivity in time indicates that the concrete permeability is decreasing, and hence, indicates the influence of LWFA on hydration of concrete.

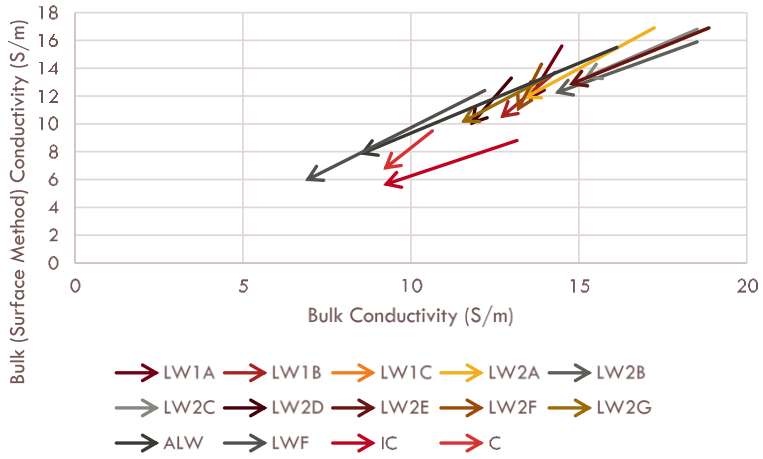

FIGURE 19 COMPARISON OF SURFACE CONDUCTIVITY (1/SURFACE RESISTIVITY) TO BULK CONDUCTIVITY FROM 28- TO 90-DAY AGES

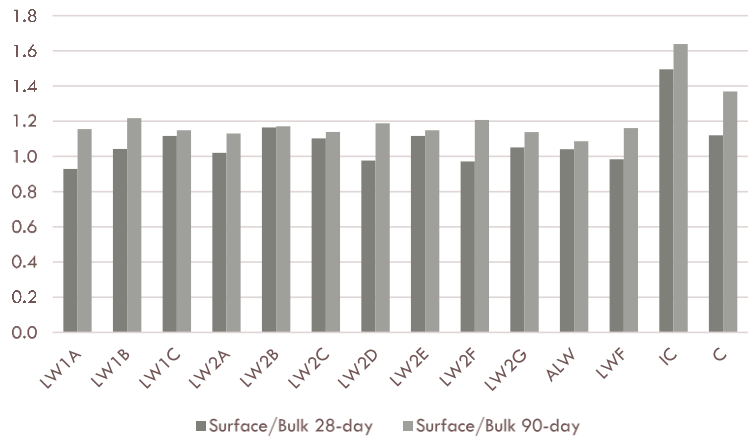

FIGURE 20 SURFACE-TO-BULK CONDUCTIVITY RATIO

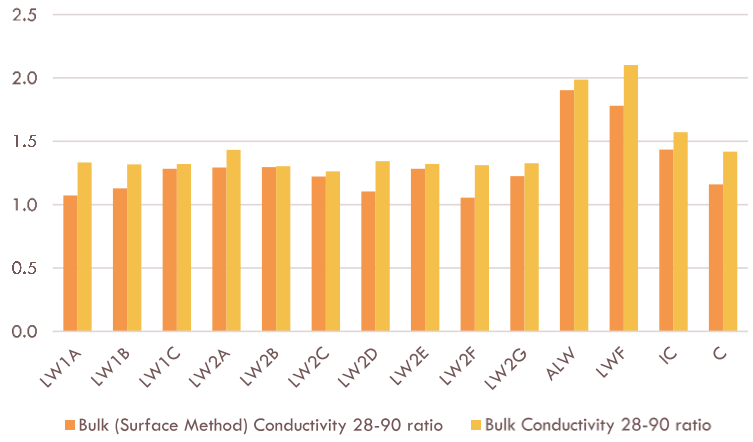

FIGURE 21 28-TO-90-DAY CONDUCTIVITY RATIO

Figure 22 exhibits the relationship between porosity and conductivity of various mixtures. Trend lines in this figure indicate that conductivity typically drops with the increase in the permeable voids, even though, the confidence level of the relationship is not appropriate for a high fidelity fit.

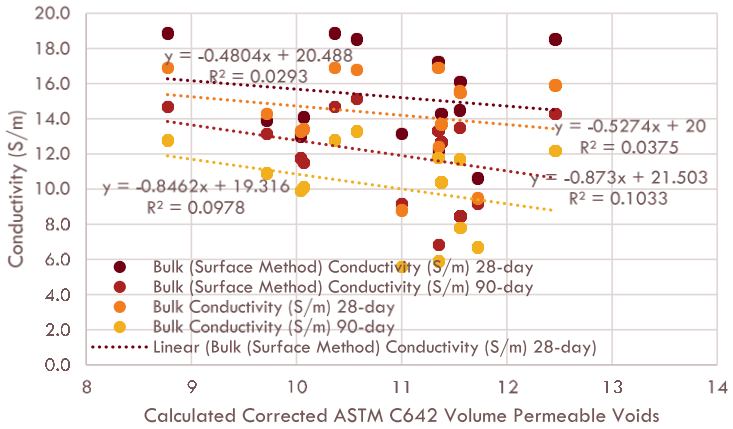

FIGURE 22 POROSITY - CONDUCTIVITY RELATIONSHIP

Figure 23 exhibits similar relationship between porosity and conductivity changes of various mixtures. Presented trend lines hint toward slight increase in surface-to-bulk conductivity ratios as the porosity increases. The same applies to the change in conductivity from 28- to 90-day ages. Regardless, the small R-square values indicate that such relationship is loose and hence, the established observations for conductivity changes are not biased by the volume of permeable voids in each mixture.

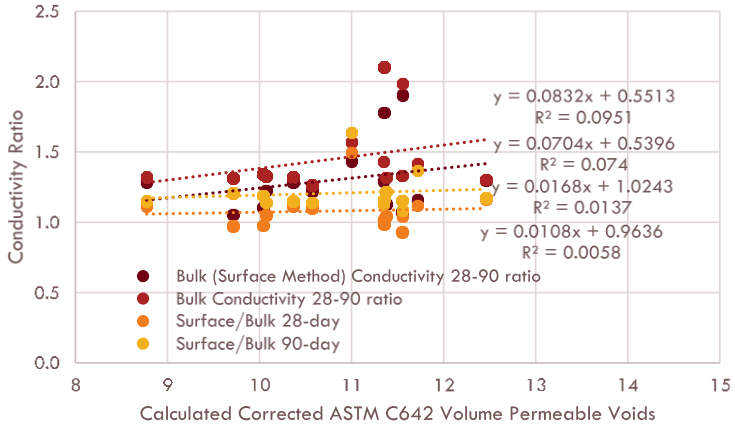

FIGURE 23 POROSITY - CONDUCTIVITY RATIO RELATIONSHIP

Table 7 provides the transport properties for application in the Life 365™ and similar models that do not directly address chloride bonding, movement of other ions, and chemical reactions occurring in concrete over time. These properties include either the ASTM C1556 bulk diffusion coefficient or the NT Build 492 non-steady state diffusion coefficient, and the ASTM C1585 Absorption [63-65].

TABLE 7 STATISTICAL MEASURES OF TRANSPORT PROPERTIES FOR USE IN LIFE 365™

Transport Property	LW1 Mean	LW1 Std. Dev.	LW2 Mean	LW2 Std. Dev.	ALW	LWF	IC	C
Nordtest NT Build 492 ($\mu m^2/s$) 28-d	10.7	0.7	10.8	1.0	9.4	9.6	11.6	14.7
C1152 Acid C1556 Background (ppm)	213	94	95	6.5	99	756	658	686
Diffusion ASTM C1556 (µm2/s) 28-d	4.6	0.2	4.6	0.7	4.4	1.9	4.5	3.6
Cs (ppm)	10437	1898	11974	3885	20639	21825	8430	8762
Cs (ppm) Adjusted for porosity	6117	2720	7211	1915	13829	13809	7016	8762
ASTM C1585 Initial Absorption (28-d)[1]	7.3E-04	1.8E-04	8.3E-04	3.3E-04	2.0E-04	9.4E-04	7.2E-04	8.3E-04
ASTM C1585 Secondary Absorption (28-d)[1]	2.5E-04	3.7E-05	3.0E-04	6.3E-05	4.0E-05	3.7E-04	3.4E-04	3.5E-04
ASTM C1585 Initial Absorption (90-d)[1]	4.4E-04	2.3E-04	5.2E-04	2.5E-04	3.3E-04	2.3E-04	4.4E-04	7.7E-04
ASTM C1585 Secondary Absorption (90-d)[1]	2.2E-04	5.8E-05	1.8E-04	7.3E-05	1.7E-04	2.8E-04	3.1E-04	3.7E-04
Nordtest NT Build 492 (pm2/s) 28-d	0.73	0.05	0.74	0.07	0.64	0.65	0.79	1.00
Diffusion ASTM C1556 (pm2/s) 28-d	1.27	0.05	1.27	0.19	1.22	0.53	1.25	1.00

[1] ASTM C1585 data are in $mm/s^{0.5}$

As shown in Figure 24, the NT Build 492 and ASTM C1556 values follow the same trend, but the ASTM bulk diffusion values are lower. This is related to the 35 days of additional ponding for the ASTM specimens in the NaCl solution as well as the NT Build 492 being a non-steady-state value. In a few cases NT Build 492 was conducted at 90 days and the values were still higher than those of ASTM C1556 at a combined 63 days of moisture (28-day fog room and 35-day ponding), so it appears that NT Build 492 might provide too high a value, but this can be correlated to ASTM C1556, as are the ASTM C1202 or ASTM C1760 test results [61-64].

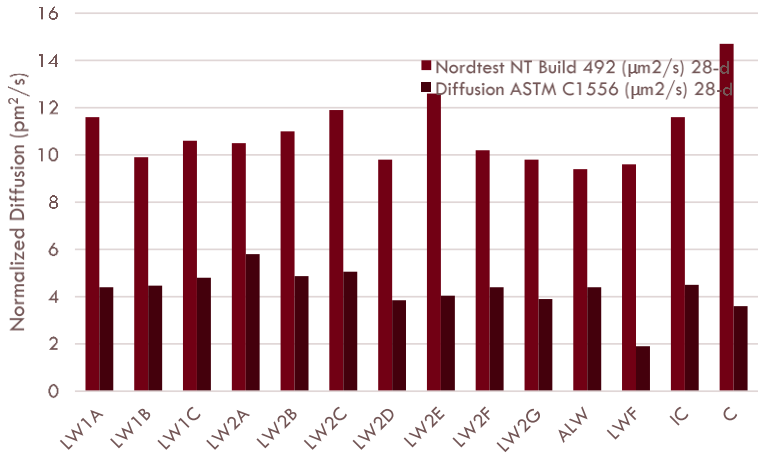

FIGURE 24 CHLORIDE DIFFUSION COEFFICIENT

The NT Build 492 test method has one advantage over other accelerated test methods in that it cancels out the effects of higher conductivity, which would be present if salts or porous lightweight aggregate were present. It shows that the non-steady state diffusion coefficient is lowered when LW aggregates are used. The chloride front is not as deep for the same potential or current range as chlorides are filling the aggregates and not penetrating as far. Figure 25 shows the cells used for the NT Build 492 test. They are like the more familiar ASTM C1202 cells, with the key feature being a much larger reservoir of solutions on both ends. Figure 25 also shows the process of breaking open the specimens for NT Build 492 and applying $AgNO_3$ to determine the depth of the chloride front [62-63].

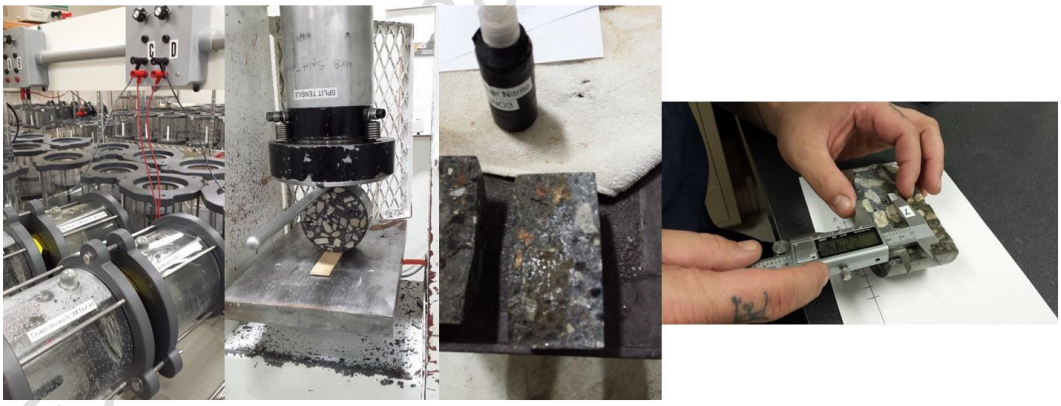

FIGURE 25 TEST CELLS FOR NT BUILD 492 (LEFT), IDC SPECIMENS (CENTER LEFT), AND PROCEDURE TO DETERMINE CHLORIDE FRONT IN NT BUILD 492 (CENTER RIGHT AND RIGHT)

The ASTM C1556 bulk diffusion data show that all of the concretes except for LWF have similar bulk diffusion coefficients even with the much higher porosities for the LWA (Figure 26 and Figure 27). As shown in Figure 28, the calculated surface concentration (Cs) is higher for the LW mixtures as would be expected for the presence of porous aggregates. A Cs value adjusted for the aggregate porosity is shown as well. The concretes with LW sand tend to show higher values as noted earlier, indicating that the sand might have a higher porosity than estimated. The values are based upon mass of concrete, so as the LW mixtures have a lower unit weight, actual chloride contents in mass/unit volume are lowered. The porosities and mass corrections will be accounted for in the Life 365™ modeling.

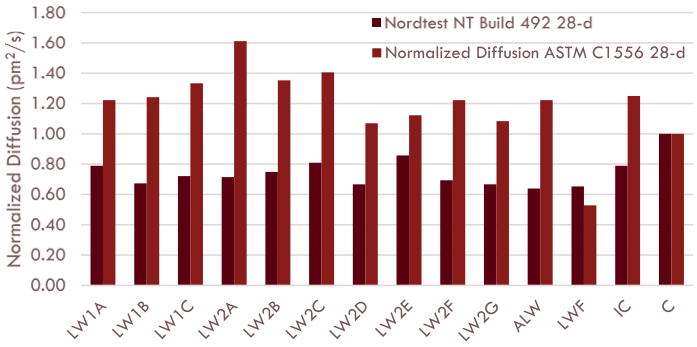

FIGURE 26 NORMALIZED CHLORIDE DIFFUSION COEFFICIENT

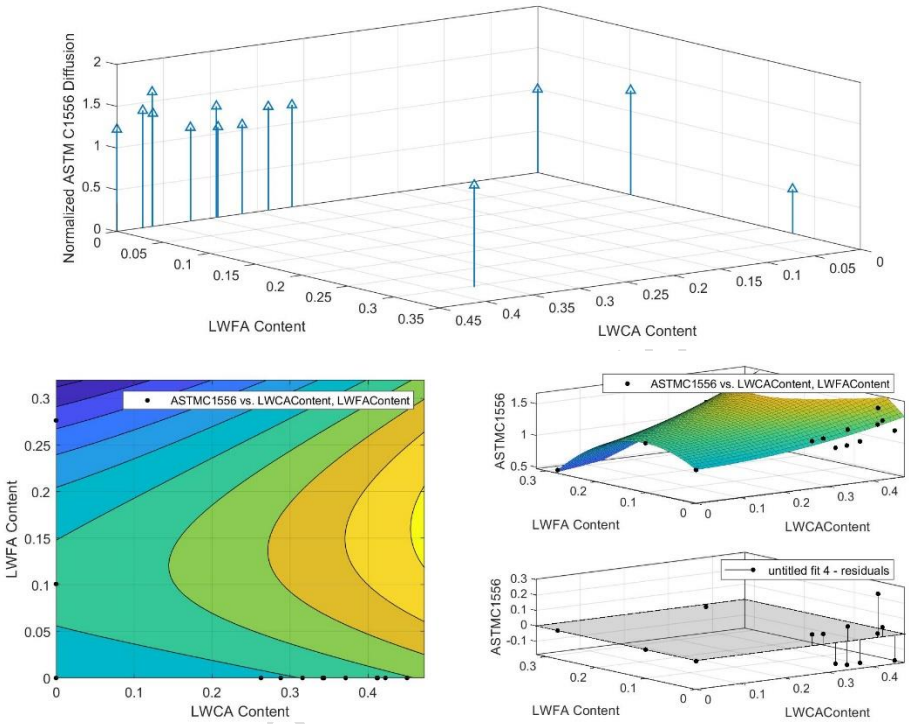

FIGURE 27 TRENDS OF ASTM C1556 DIFFUSION RESULTS AT 28-DAY (TOP), FITTING PLANE (MIDDLE), CONTOURS (BOTTOM LEFT), AND ERROR (BOTTOM RIGHT)

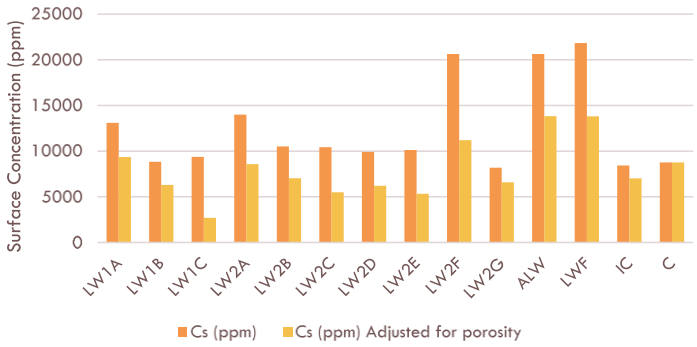

FIGURE 28 SURFACE CONCENTRATION

The ASTM C1585 absorption data in Table 7 show that LW concrete mixtures have lower average absorption than NW concrete mixtures of the same design, even though, comparisons in Figure 29 and Figure 30 reveal that this observation is not applicable to all LW mixtures. Presented data in Table 7 exhibit high measures of deviation in recorded absorptions for LW1 and LW2 mixtures at both 28-day and 90-day ages, particularly for initial absorptions. Moreover, it is also evident from Figure 30 that the initial absorption of ALW mixture at 28 days and LWF mixture at 90 days are lower than expected. Regardless, this observation contrasts with the higher porosity of LW aggregates. The specimens are conditioned in an 85% relative humidity (RH) environment at elevated temperature versus above the boiling point of water. The results indicate that at 85% RH the pores in the aggregates do not absorb moisture quickly. The 85% RH value was chosen for the ASTM method as it results in internal RH values for concrete mixtures that are like those exposed to environments with deicing or marine salts. Thus, in applications where corrosion is an issue, these tests show that there is a significant reduction in absorption with LW aggregate. This will be accounted for in the Life 365™ modeling by increasing the time to reach the maximum chloride concentration at the surface.

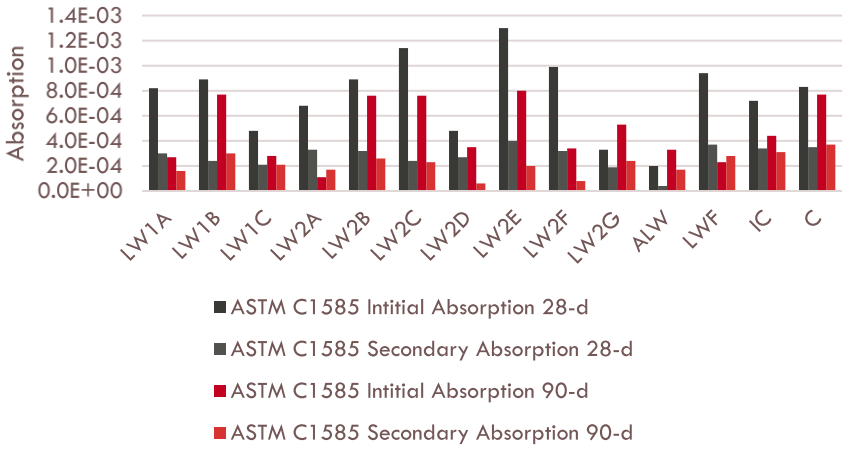

FIGURE 29 ASTM C1585 ABSORPTION DATA

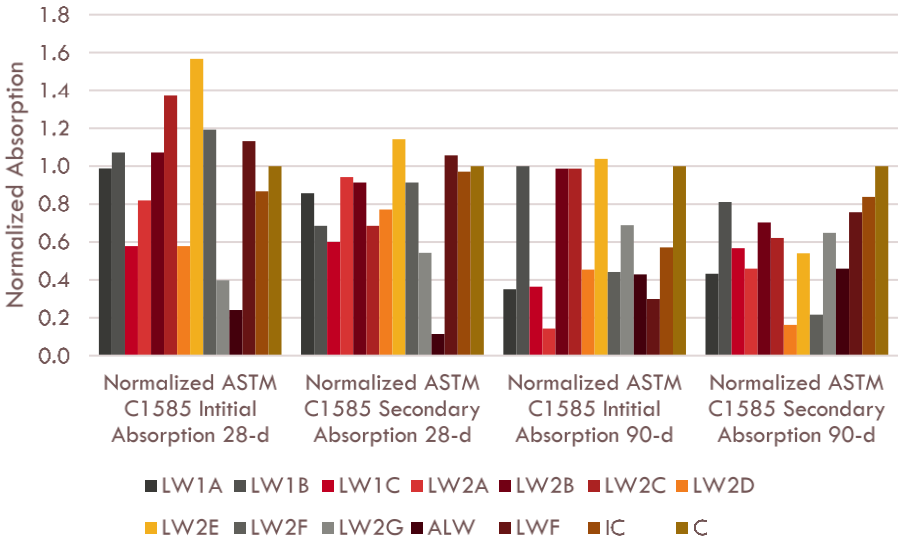

FIGURE 30 NORMALIZED ASTM C1585 ABSORPTION DATA

Table 8 presents transport properties and their statistical measures for application in STADIUM®. According to average results, the ionic diffusion coefficient (IDC) of mixtures are like each other for LW1 and LW2 mixtures, while

the mixtures with fines, IC, LWF, and ALW, have lower values as seen for the bulk diffusion data. However, detailed individual results indicate that the LW2 mixtures have substantially larger coefficient of variation than LW1 mixtures, which might be correlated to the sizes of the population in each group. Figure 31 and Figure 32 exhibit that LWFA have more influence on reduction of IDC than LWCA. It is also notable that certain individual mixtures containing LWCA had higher IDC values than the control mixture. Figure 33 and Figure 34 provide insights on moisture transport coefficient (MTC) data. The MTC values are very high for the LW aggregate concrete mixtures. This would normally indicate that they have much higher sorption properties than the control mixture, which is not a good property in wetting and drying applications as in bridge and parking decks, or airborne exposures. This was in contrast to the ASTM C1585 absorption data, as shown in Figure 35 and three-dimensional models in Figure 36 and Figure 37. The apparent reason is that drying at 50% RH might not be representative of the field conditions, and it is more difficult for LW concrete mixtures to absorb water back at higher RH. As noted earlier, this is due to more difficulty in reabsorption of water into the lightweight aggregate. Significantly less water is being absorbed than is indicated by the MTC values. The MTC value for the control mixture C will be multiplied by the ratio of the initial absorption of the LW mixtures to the control mixture to provide a modified MTC for the LW mixture, and hence, the MTC value will be directly related to the initial absorption rate. In most cases as can be seen in Figure 35, the LW will have a modified MTC that is equal to or lower than laboratory data, particularly for 90-day results. Regardless, error plots in Figure 36 and Figure 37 reveal an underlying issue with the accuracy of MTC values for individual mixtures. A close look at the ratio of 28-day MTC to 90-day MTC for various mixtures highlights the uncertainties associated with the MTC measurement.

TABLE 8 AVERAGE STADIUM® TRANSPORT DATA

Transport Property	LW1 Mean	LW1 Std. Dev.	LW2 Mean	LW2 Std. Dev.	ALW	LWF	IC	C
IDC 28 Day (µm2/s)	125.8	5.9	116.5	19.7	98	72	104	142.8
IDC 90 Day (µm2/s)	101.9	7.6	90.6	14.0	71	42	78	97.5
MTC at 28 Day (pm2)	6584	437	11734	5483	15430	4640	2200	1000
MTC at 90 Day (pm2)	8614	2546	9105	3918	9860	2250	1590	868

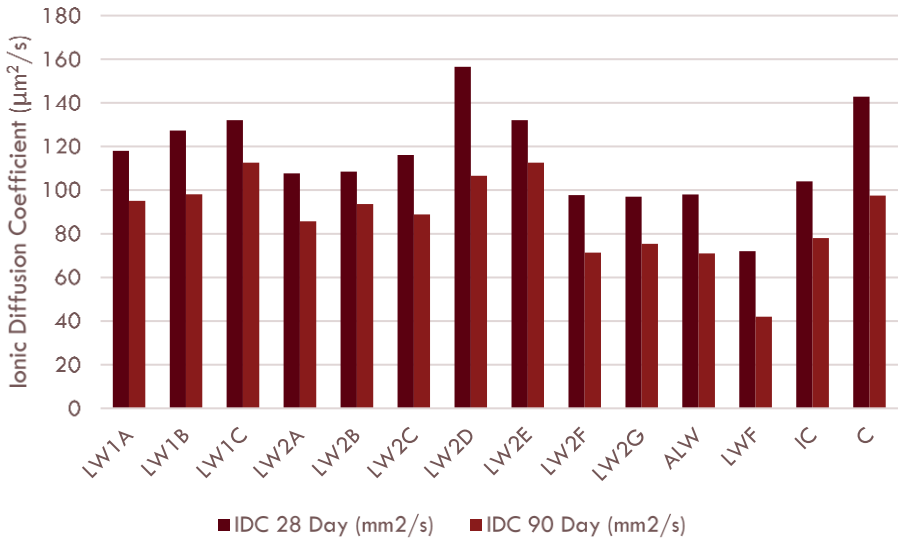

FIGURE 31 IDC DATA

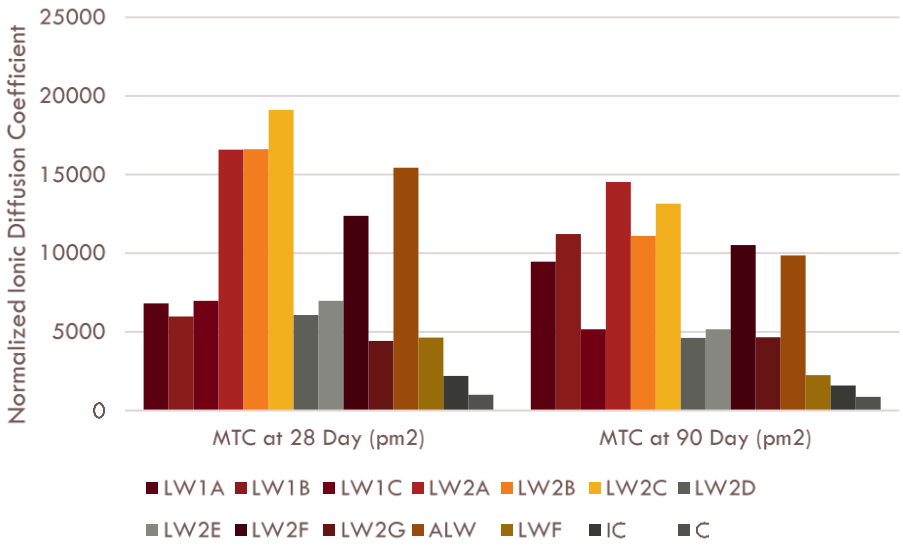

FIGURE 32 NORMALIZED IDC DATA

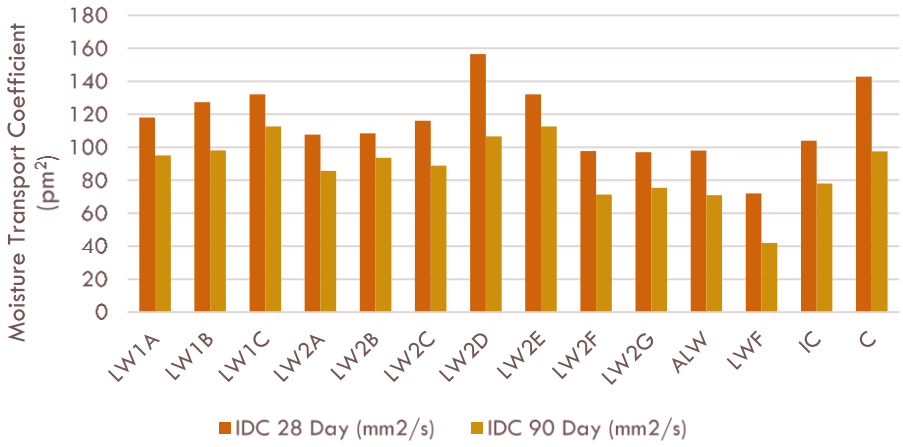

FIGURE 33 MTC DATA

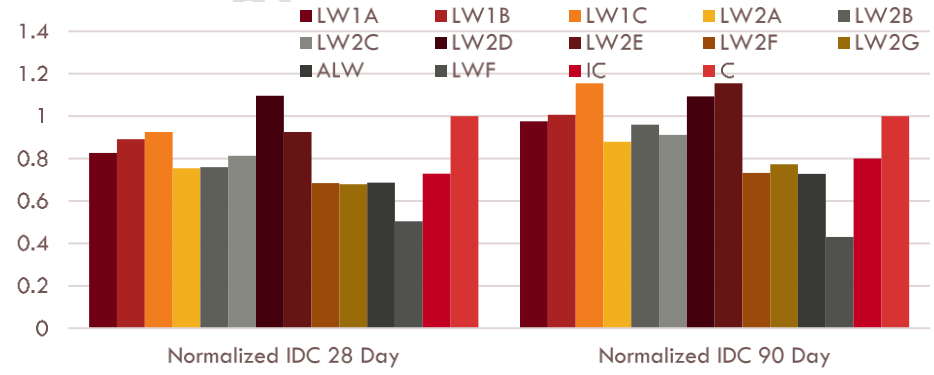

FIGURE 34 NORMALIZED MTC DATA

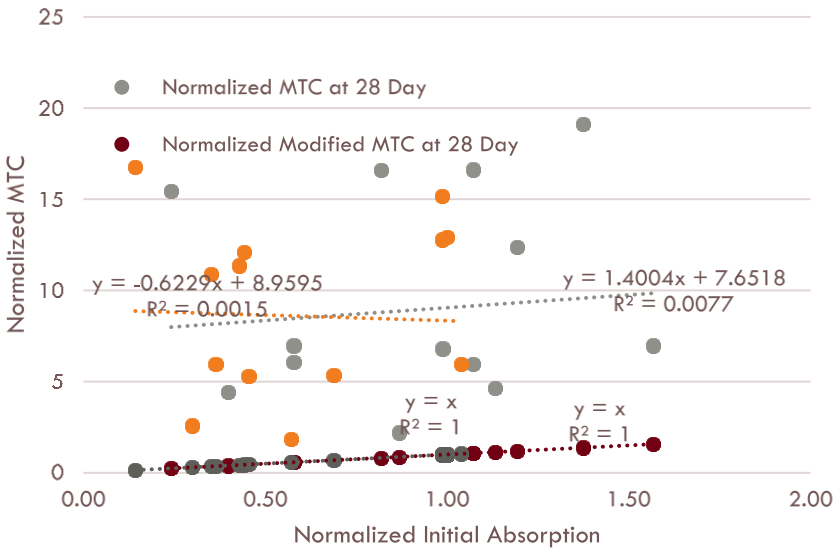

FIGURE 35 CONTRAST BETWEEN ASTM C1585 ABSORPTION AND MOISTURE TRANSPORTATION DATA

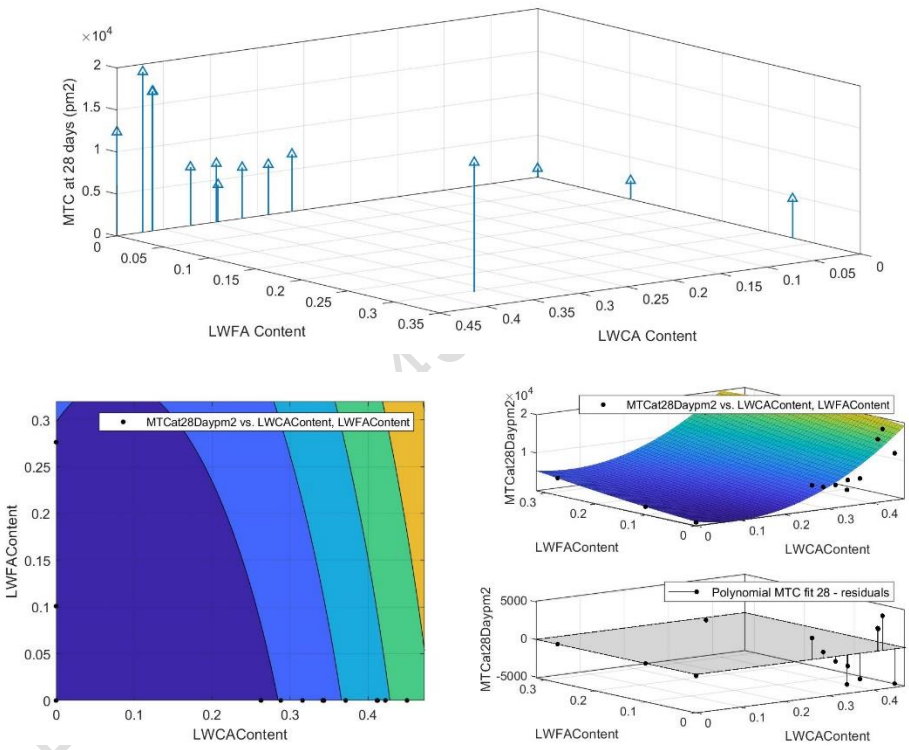

FIGURE 36 TRENDS OF MTC AT 28-DAY (TOP), FITTING PLANE (MIDDLE), CONTOURS (BOTTOM LEFT), AND ERROR (BOTTOM RIGHT)

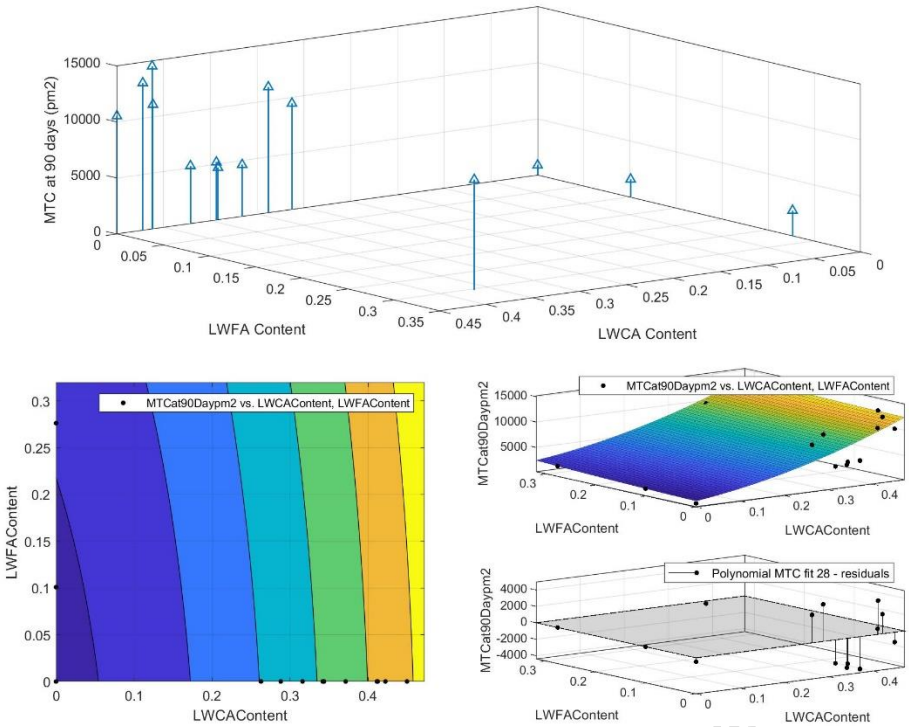

FIGURE 37 TRENDS OF MTC AT 90-DAY (TOP), FITTING PLANE (MIDDLE), CONTOURS (BOTTOM LEFT), AND ERROR (BOTTOM RIGHT)

Cracking of high-performance concrete mixtures in the field is a major concern. The concrete mixtures in this study had a water-cementitious-materials-ratio (w/cm) below 0.4 and were susceptible to restrained drying shrinkage cracking from both autogenous and normal drying shrinkage processes. The ASTM C1581 restrained shrinkage ring tests [66] were conducted on the control mixture C, and the internally cured mixture IC which had portion of NWFA replaced with LWFA. The ratio of the substitution was based on the ESCSI recommendation [76]. Figure 38 and Figure 39 show the restrained shrinkage stresses as a function of time for these two mixtures. Figure 40 shows a cracked control ring specimen.

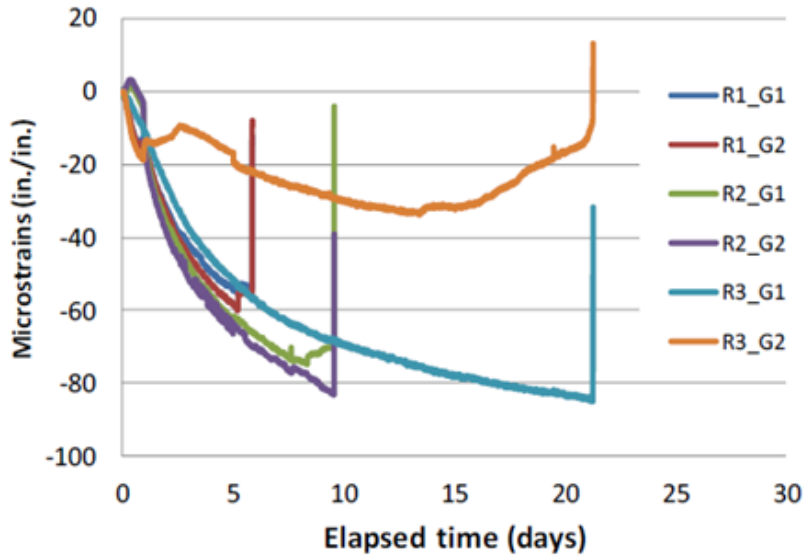

FIGURE 38 ASTM C1581 STRAIN (STRESS) DATA FOR CONTROL MIXTURE C RINGS

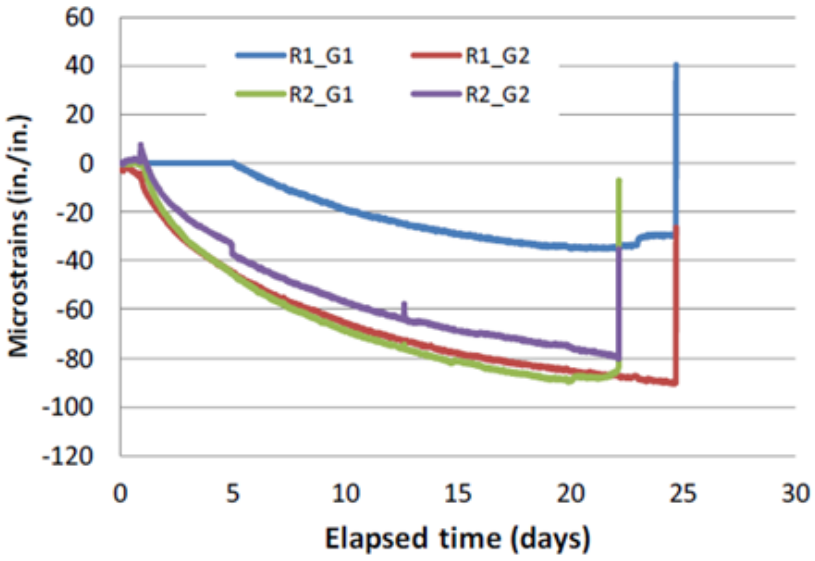

FIGURE 39 ASTM C1581 STRAIN (STRESS) DATA FOR INTERNAL CURING MIXTURE IC RINGS

FIGURE 40 IMAGE OF A CRACKED CONTROL ASTM C1581 RESTRAINED SHRINKAGE SPECIMEN

Table 9 summarizes the cracking performance of mixtures. These data show an improvement in the time to cracking and a reduction in the shrinkage stress by 46% with the application of the LWFA in mixture IC. The mixture C is classified as a mix with moderate-high probability of restrained shrinkage cracking, whereas the mixture IC is classified as a mix with moderate-low probability of restrained shrinkage cracking.

TABLE 9 ASTM C1581 RESTRAINED SHRINKAGE RING RESULTS

Property	IC Mean	IC Std. Dev.	C Mean	C Std. Dev.
Initial Strain (με)	-1	5.4	-13.2	1.4
Maximum Strain (με)	-74	26.2	-65.4	19.5
Strain at Cracking (με)	-70.8	28.1	-58.5	28.9
Age at Cracking (days)	22.2	1.8	12.2	8
Stress Rate (psi/day)	18	4.5	33.5	17.3

2. Service Life Analysis

Service life analysis utilized simulations by Life 365™ and STADIUM®. These simulations follow the basic guidelines in the *fib* Bulletin 34 [24, 28, 45]. The simulation modeled a bridge deck subjected to deicing salts in Detroit, MI. Typically, a less permeable mixture containing SCMs would be applicable in this case, however, this study considered only ordinary Portland cement (OPC) to highlight the effects of the LW aggregate for a low w/cm mixture.

Life 365™ Service Life Analysis

The default values in the Life 365 program for a Detroit urban bridge deck were used for the temperature data. Concrete cover was chosen to be 75 mm (3 inches) in the absence of SCMs or additional corrosion protection. The 28-day ASTM C1556 bulk diffusion values were obtained from experimental results, which were lower than default values in Life 365™. The default rate of chloride ingress was modified for the LW mixtures by multiplying the years of buildup for the control mixture by the ratio of the control ASTM C1585 initial absorption to the LW initial absorption at 90 days. The buildup time for the control mixture was multiplied by an additional 2.5 times to account for the ratio of the control at 28 days to that of a typical concrete at 28 days at a higher w/cm. Figure 41 exhibits the relationship between these parameters and highlights the deviations of results for certain mixtures from the overall trend. The mixture design data resulted in lower capillary absorption values for typical mixtures upon which the data in Life 365™ were determined. The Life 365™ model does not directly address porosity which would lead to higher actual chloride concentrations at all levels. Since this chloride is in the porous aggregates and not the paste, it does not contribute to the corrosion. Therefore, a correction is not needed for modeling corrosion performance. However, due to the higher porosity, the measured surface concentration is higher. This increase is subject to correction for determining the threshold value. Note that the maximum chloride content at the surface is the 0.85% on concrete in the Life 365™ model multiplied by the ratio of the *Cs* value of the lightweight mixture to that of the control mixture.

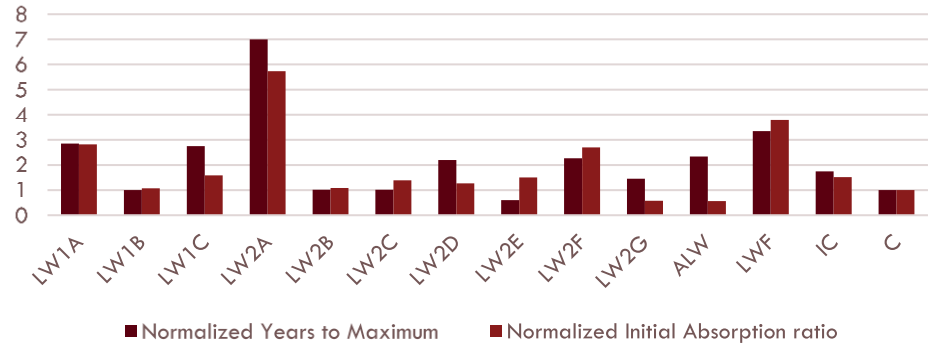

FIGURE 41 NORMALIZED YEARS TO MAXIMUM AND INITIAL ABSORPTION RATIO

Table 10 provides diffusion values along with other modeling parameters in the Life 365™. The diffusion coefficient will decrease in time due to continued cement hydration. The *m* parameter as defined below is used to develop the relationship of the diffusion coefficient to time. The *m* values were determined by comparing the ASTM C1760 bulk conductivity values at 28 and 90 days and fitting it to the equation:

$$\kappa_{90} = \kappa_{28}(t_{28}/t_{90})^m$$

where, κ_t is the conductivity at time *t*, and *m* is the aging (hydration) coefficient. As the conductivity is directly related to the diffusion coefficient, the *m* value calculated describes how the diffusion coefficient will decrease in time according to the equation:

$$D_t = D_{28}(28/t)^m$$

where D_t is the diffusion coefficient at time *t*. The default value for the *m* parameter in Life 365™ is 0.2 for Portland cement. Since only Portland cement is present, the diffusion coefficient was assumed to become constant after one year [77-80]. Longer curing times could be used to determine if hydration continues for longer periods with lightweight aggregates. Figure 42 presents the normalized diffusion and *m* values, indicating the conceptual

difference between the effects of LWCA and LWFA. Figure 43 highlights these effects and high deviant points for high LWCA content mixtures.

TABLE 10 PARAMETERS IN THE LIFE 365™ MODEL

Transport Property	LW1 Mean	LW1 Std. Dev.	LW2 Mean	LW2 Std. Dev.	ALW	LWF	IC	C
Diffusion ASTM C1556 (E-9 in²/s) 28-d	7.06	0.27	7.07	1.04	6.82	2.95	6.98	5.58
m	0.24	0.004	0.24	0.031	0.59	0.64[1]	0.39	0.30
Hydration Time (Years)	1	0	1	0	1	1	1	1
Maximum Surface Concentration (% mass)	1.01	0.184	1.16	0.377	2.00	2.12	0.82	0.85
Years to Maximum	34.1	13.2	35.2	31.0	36.2	51.9	27.1	15.5
Chloride Threshold (% mass)	0.13	0.064	0.10	0.015	0.10	0.09	0.06	0.05

[1] Maximum allowed m in Life 365™ is 0.6

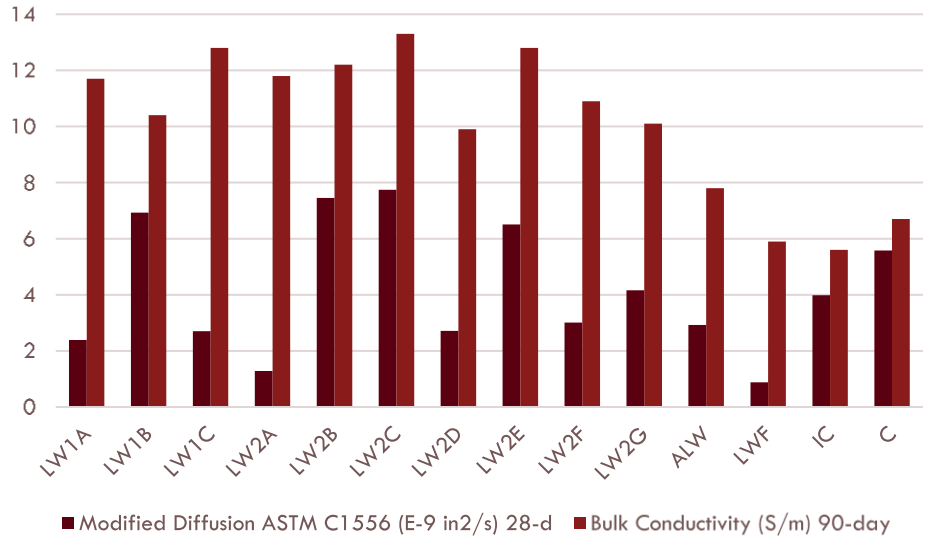

FIGURE 42 COMPARISON OF DIFFUSION AND CALCULATED RATE OF CONDUCTIVE IN TIME, *M* VALUE

The last correction that needs to be made for Life 365™ is to adjust the corrosion threshold levels. The Life 365™ assumes the same unit weight for all concrete mixtures. This is not the case for this study, thus, there is a need to multiply the chloride threshold level, *Ct* by the unit weight of the control concrete divided by that of the lightweight concrete. This number is multiplied again by the ratio of the determined surface chloride to the corrected surface value. This correction results in higher threshold values for the lightweight concrete mixtures reflecting that some chloride is not available and that the mass of the concrete is lower, even though the cement content is the same as the control mixture.

The performed service life analysis considers a comparison between the control NW aggregate mixtures and similar LW aggregate mixtures utilizing the same design approach to address the effects of the aggregate porosity on the outcome.

The target service life was defined as 6 years after the onset of corrosion in the Life 365™ model. Table 11 shows the resulting service lives and their statistical trends. Curves for chloride as a function of time until corrosion initiation at 75 mm (3 inch) level and service life graphs are available in Figure 46 to Figure 53. Note that the Life 365™ does not adjust for the unit weight, therefore, the chloride threshold values on mass of concrete would be higher than what

is shown in these curves, which explains the increased threshold level. The chloride in the LW aggregate is accounted for in the higher surface concentration.

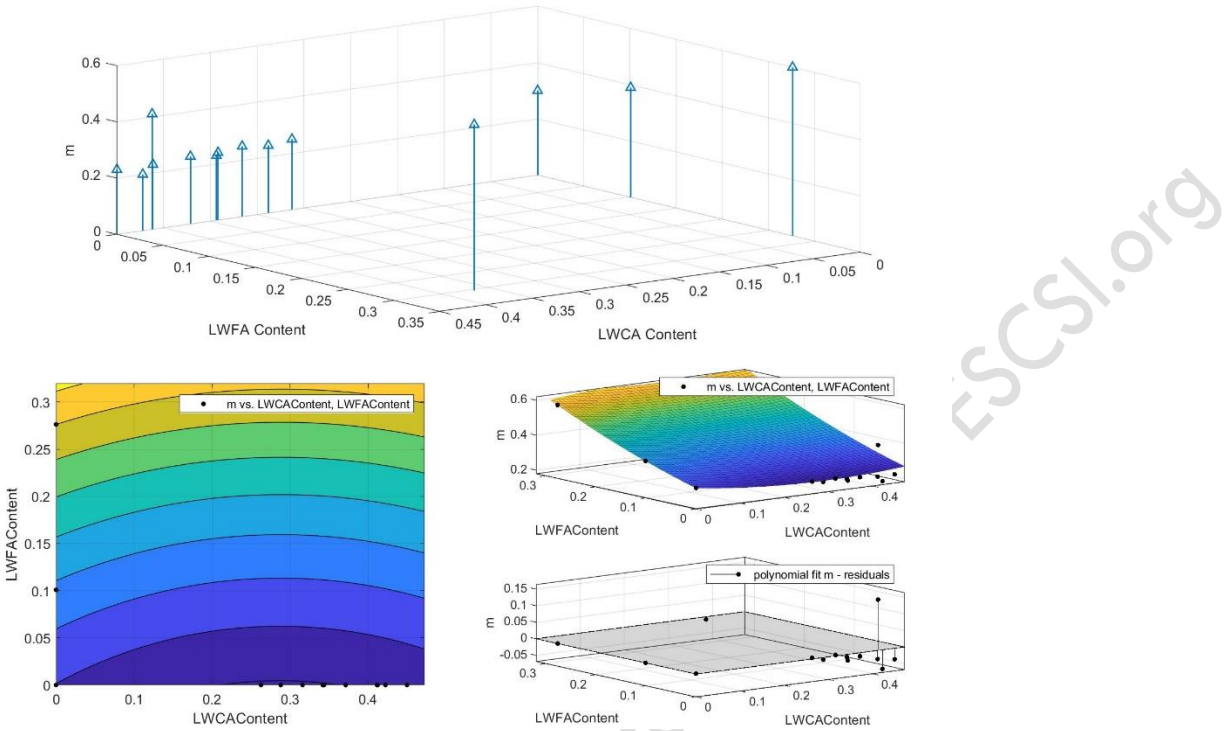

FIGURE 43 TRENDS OF M CONSTANT (TOP), FITTING PLANE (MIDDLE), CONTOURS (BOTTOM LEFT), AND ERROR (BOTTOM RIGHT)

The Life 365™ analysis reveals that the performance of the LW mixtures varies among different mixtures with a range of 0.86 to 1.64 times the control NW mixture, with 34% and 15% increase for LW1 and LW2 mixtures, respectively. This is even though the conductivity is higher for the LW mixtures and more chloride would be in the concrete due to porosity in the aggregates. However, as shown in Table 11, there is a significant improvement in the ALW and LWF mixtures of approximately 1.64 to 3.06 times (64% to 206% increase), indicating that increasing the LWFA content is an effective means of increasing the service life of the concrete. The addition of LWFA for internal curing results in approximately a 25% improvement in service life predictions. A conservative approach of one year for hydration to continue was used; if it continued longer, then the service life would be higher. This is especially the case for the concrete mixtures containing LWFA. Figure 44 provides the Life 365™ estimate of the life cycle cost using default values.

TABLE 11 AVERAGE LIFE 365™ PREDICTIONS OF SERVICE LIFE (6 YEARS AFTER CORROSION INITIATION)

Concrete	LW1 Mean	LW1 Std. Dev.	LW2 Mean	LW2 Std. Dev.	ALW	LWF	IC	C
Service Life (Years)	48	14	41	9	59	110	45	36

TABLE 12 AVERAGE LIFE 365™ PREDICTIONS OF NORMALIZED LIFE CYCLE COST

Concrete	LW1 Mean	LW1 Std. Dev.	LW2 Mean	LW2 Std. Dev.	ALW	LWF	IC	C
Normalized Life Cycle Cost	0.90	0.10	0.96	0.06	0.84	0.45	0.92	1.0

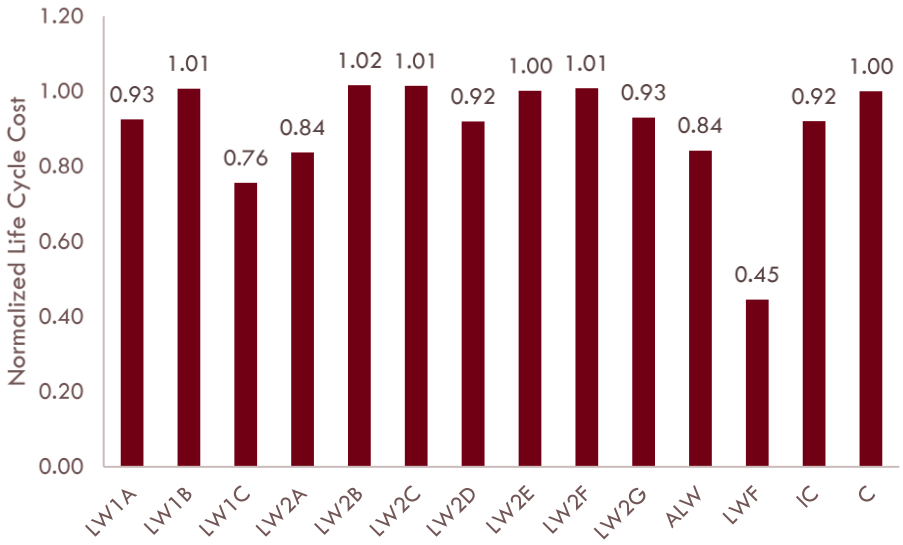

FIGURE 44 NORMALIZED LIFE CYCLE COST PREDICTION IN LIFE 365™

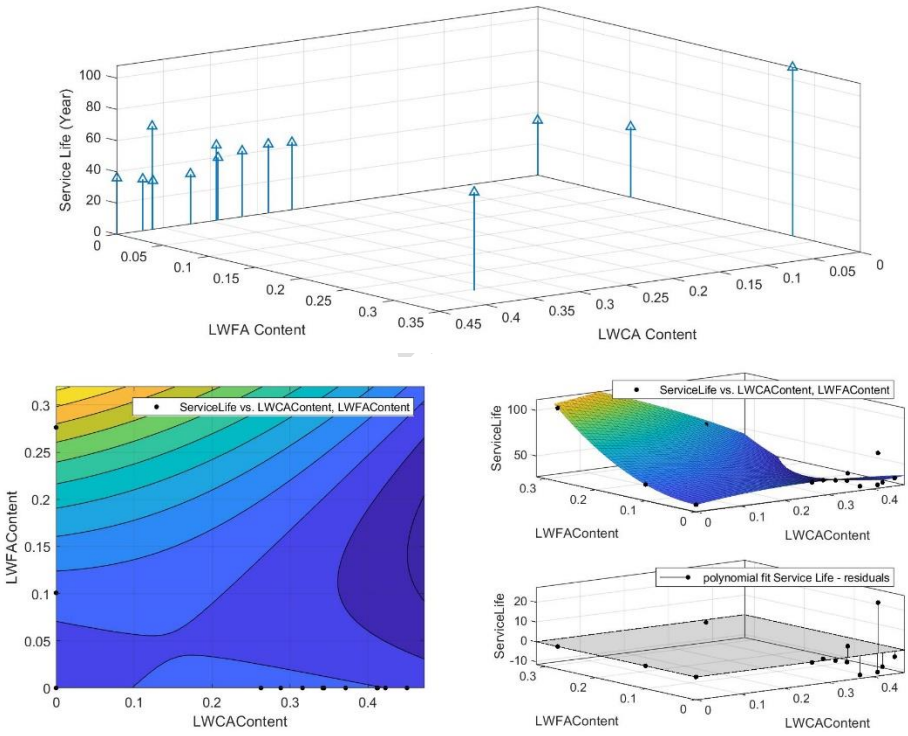

FIGURE 45 TRENDS OF LIFE 365™ SERVICE LIFE (TOP), FITTING PLANE (MIDDLE), CONTOURS (BOTTOM LEFT), AND ERROR (BOTTOM RIGHT)

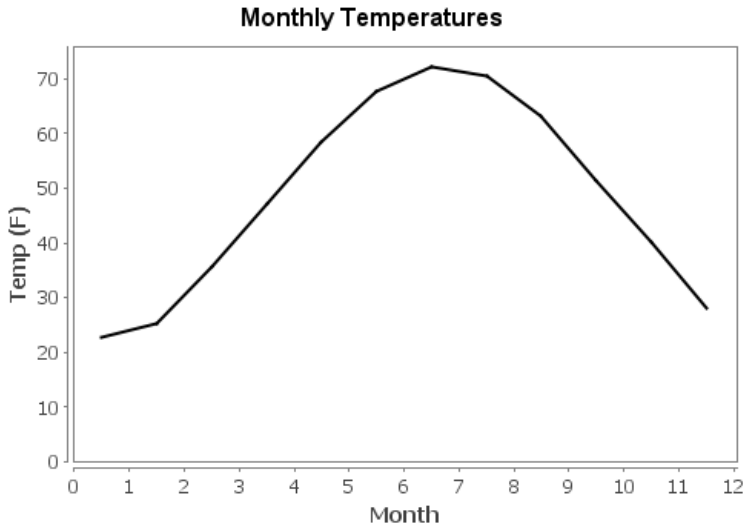

FIGURE 46 MONTHLY TEMPERATURES FOR DETROIT, MI

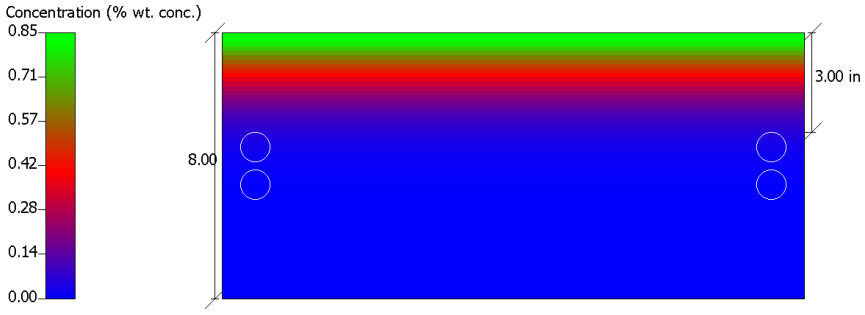

FIGURE 47 CONCENTRATION DIAGRAM FOR THE DESIGN CROSS SECTION WITH MIXTURE C

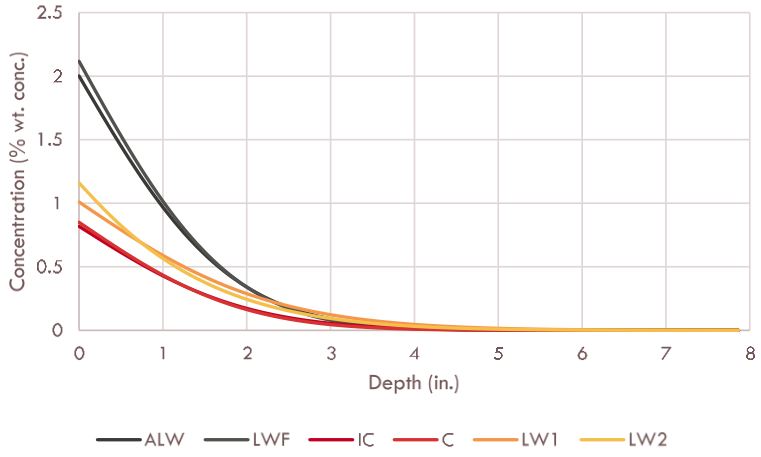

FIGURE 48 CONCENTRATION VERSUS DEPTH

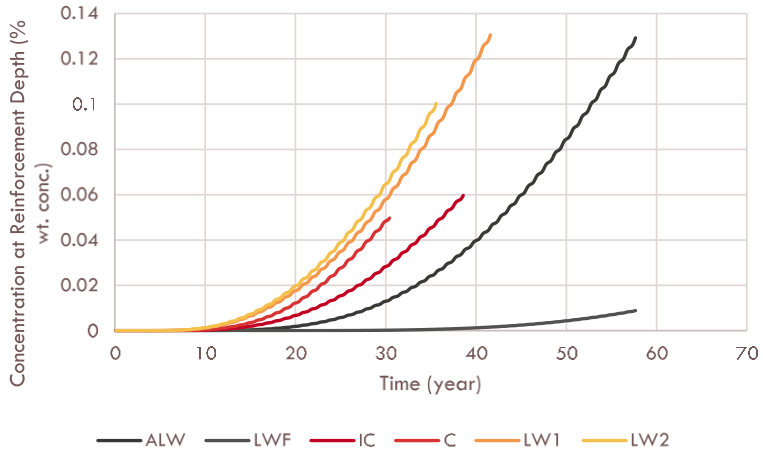

FIGURE 49 CONCENTRATION VERSUS TIME AT REINFORCEMENT DEPTH

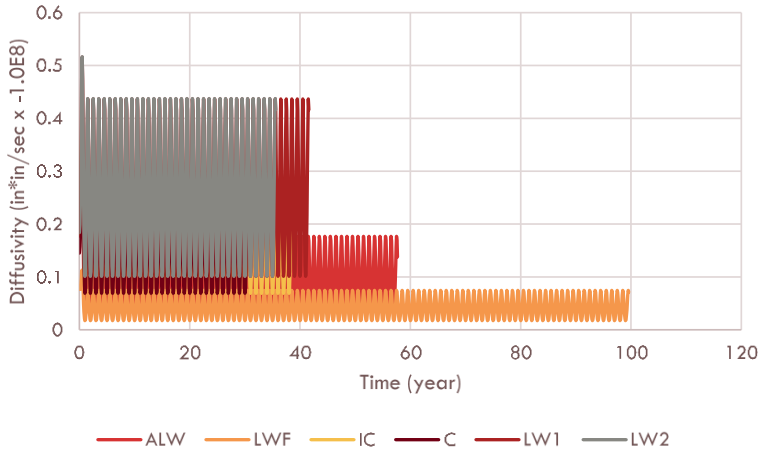

FIGURE 50 DIFFUSIVITY VERSUS TIME

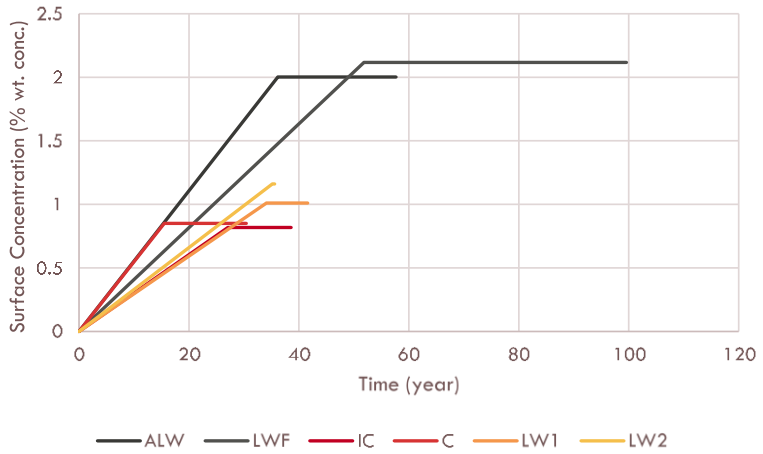

FIGURE 51 SURFACE CONCENTRATION VERSUS TIME

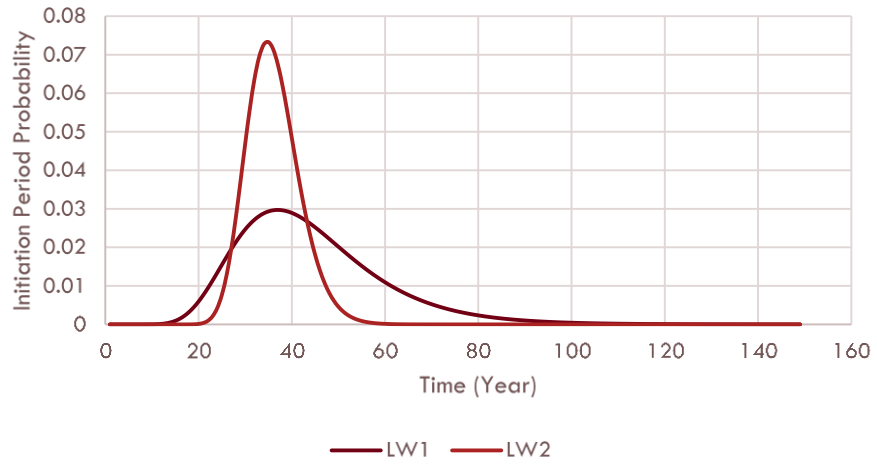

FIGURE 52 INITIATION PERIOD PROBABILITY

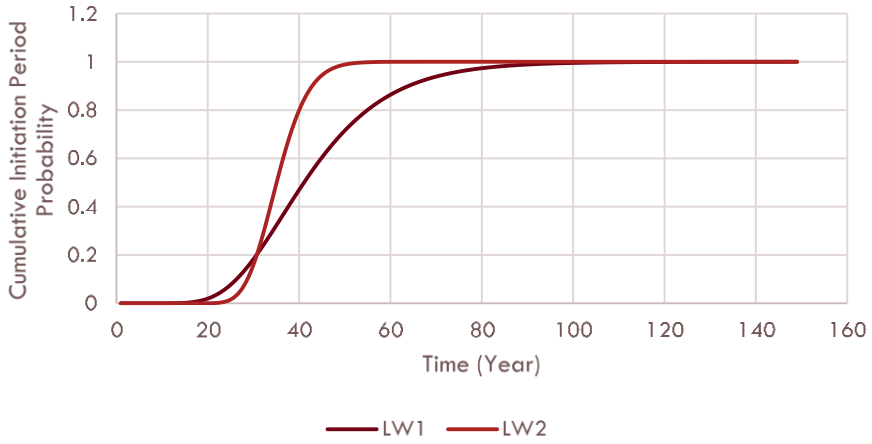

FIGURE 53 CUMULATIVE INITIATION PERIOD PROBABILITY

Following climate date by FHWA [81], the service life prediction may cover four climate zones. Figure 54 and Figure 55 exhibit a summary of normalized service life prediction results for representative cities in these climate zones: Detroit, MI (wet freezing), New Orleans, LA (wet non-freezing), San Francisco, CA (dry non-freezing), and Denver, CO (dry freezing). These results confirm previous results in effectiveness of LWA mixtures to enhance the service life of concrete. Further, it is evident that LWA mixtures are more effective in dry zones that wet zones. In particular, the internally cured mixture had the most efficiency in the dry non-freezing zone of San Francisco, CA. In addition, results include a comparison between urban highway bridge (UHB) and marine tidal zone (MTZ) concrete in San Francisco and New Orleans. Figure 55 indicates the need for FLWA to enhance the service life of concrete in marine tidal zones.

Following cost data and assumptions provided through prior life cycle analysis studies [82], the normalized life cycle unit cost of internally cured concrete was compared with the normalweight concrete for an urban highway bridge in Dubuque, IA. The data set suggests that the repair cost of concrete, including full grinding and 10% replacement, is nearly eleven times more than the cost of construction materials. Hence, the overall life cycle cost is highly sensitive to the service life of concrete. Results indicate that application of internal curing extends the service life of concrete by 30%, and hence, reduces the life cycle cost by 5%. Every percentage of change in the cost of construction materials will change the overall cost by 0.05%, while the same amount of change in repair cost has a 0.92% effect. The one

percent change in the cost of lightweight aggregate has a negligible effect of 0.001% on the overall life cycle unit cost.

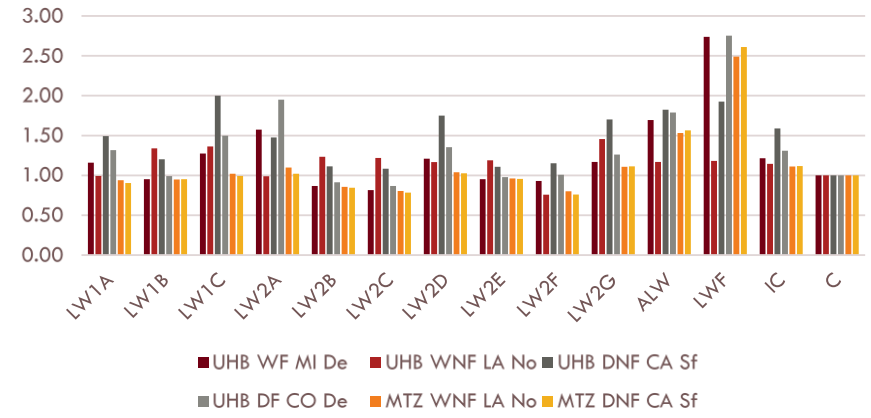

FIGURE 54 NORMALIZED LIFE 365™ PREDICTIONS OF SERVICE LIFE FOR VARIOUS CLIMATE ZONES

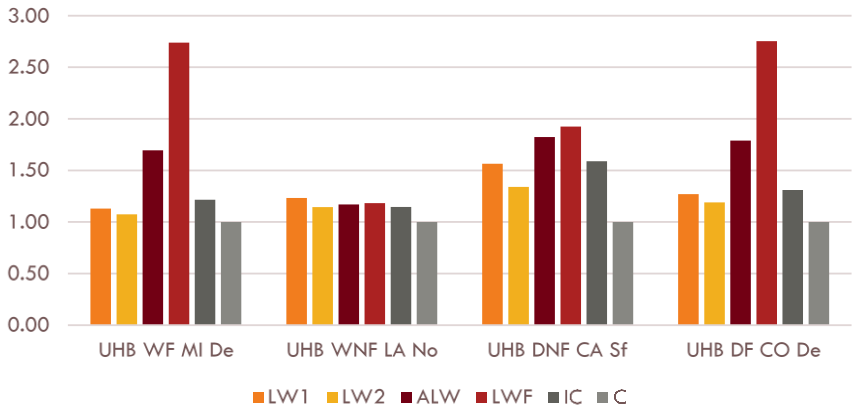

FIGURE 55 NORMALIZED LIFE 365™ PREDICTIONS OF SERVICE LIFE OF URBAN HIGHWAY BRIDGES FOR VARIOUS CLIMATE ZONES

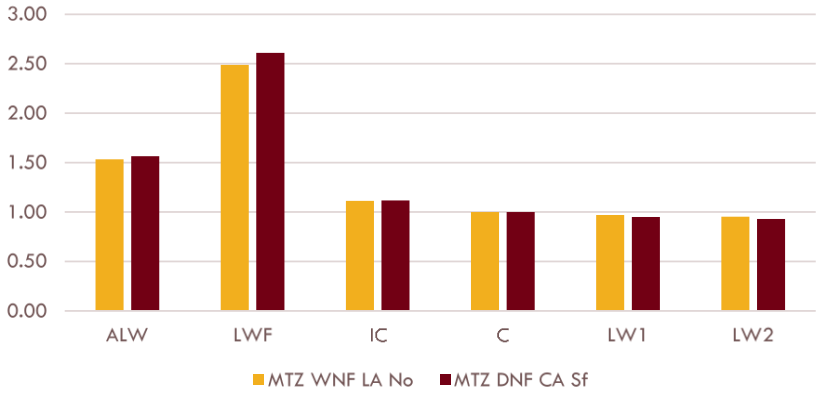

FIGURE 56 NORMALIZED LIFE 365™ PREDICTIONS OF SERVICE LIFE OF MARINE TIDAL ZONES IN LA AND CA

STADIUM Modeling

The STADIUM® simulation utilized the IDC and MTC values in Table 8. Figure 57, Figure 58, and Figure 59 exhibit the normalized values for these and other parameters in the STADIUM® model. The porosity was adjusted to reflect the porosity of the cement paste; hence, additional porosity corrections were not necessary to adjust the threshold values. In STADIUM®, the surface concentration is treated differently than in Life 365™, therefore, accessible porosity in the aggregate does not need to be addressed. To determine actual chloride content in the concrete at any given time, an adjustment is needed for porosity in the aggregate, which would raise the actual chloride level. However, this is not needed to predict the time to corrosion. As in the case for Life 365™ modeling, the threshold values are raised to reflect the lower unit weight of the concrete, however as noted, a correction for porosity is not required in STADIUM®. Table 13 shows the parameters used in the STADIUM® modeling.

TABLE 13 AVERAGE PARAMETERS USED IN STADIUM MODELING

Transport Property	LW1 Mean	LW1 Std. Dev.	LW2 Mean	LW2 Std. Dev.	ALW	LWF	IC	C
IDC at 28 days (10^{-11} m^2/s)	12.8	0.8	11.7	2.0	9.8	7.2	10.4	14.3
Hydration Parameter - a	0.52	0.02	0.42	0.10	0.44	0.39	0.39	0.39
Hydration Parameter - α (1/s)	0.0040	0.0000	0.0029	0.0014	0.0004	0.0003	0.0003	0.0004
Corrected MTC (10-22 m^2)	5.7	3.0	7.2	3.8	4.3	3.3	5.7	10
Porosity (%)	10.98	0.69	11.39	1.96	11.6	11	11.1	11.7
Max Chloride at Surface (mM/L)	1000	0	1000	0	1000	1000	1000	1000
Chloride Threshold (ppm)	777	99	824	186	700	540	515	500

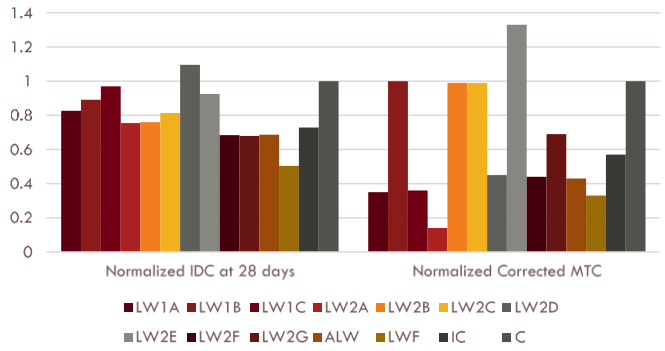

FIGURE 57 NORMALIZED IDC AND CORRECTED MTC

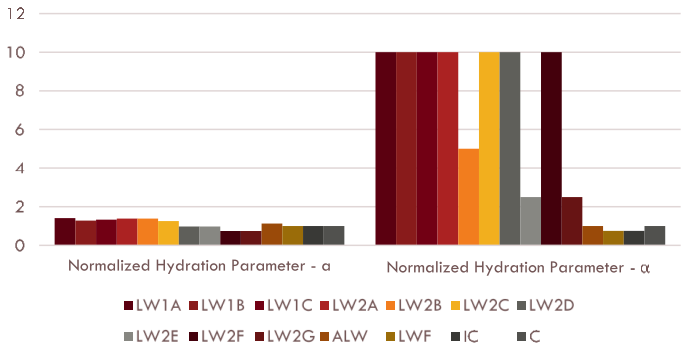

FIGURE 58 NORMALIZED HYDRATION PARAMETERS

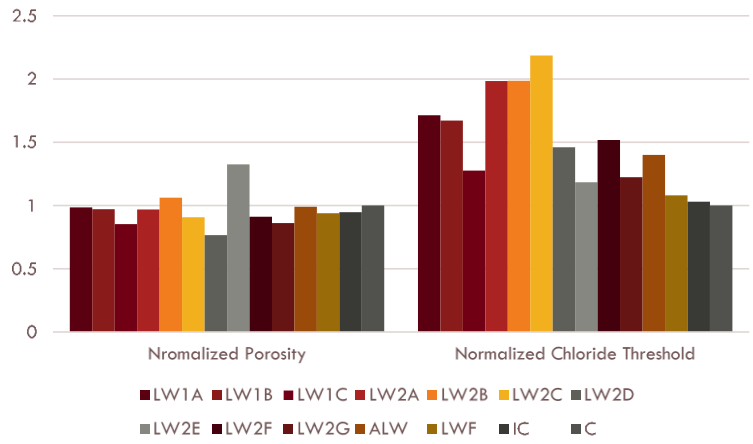

FIGURE 59 NORMALIZED POROSITY AND CHLORIDE THRESHOLD

Table 14 shows the times to spalling and cracking (initiation plus six years for propagation. Figure 60 exhibits the trend of service life for the LWCA and LWFA contents. Figure 61 presents the chloride profiles as a function of time. Note that actual chloride contents in the concrete would be higher as the chloride in the lightweight aggregate is not considered.

TABLE 14 AVERAGE STADIUM® PREDICTIONS OF SERVICE LIFE (6 YEARS AFTER CORROSION INITIATION)

Concrete	LW1 Mean	LW1 Std. Dev.	LW2 Mean	LW2 Std. Dev.	ALW	LWF	IC	C
Service Life (years)	45	3	59	11	46	64	45	34

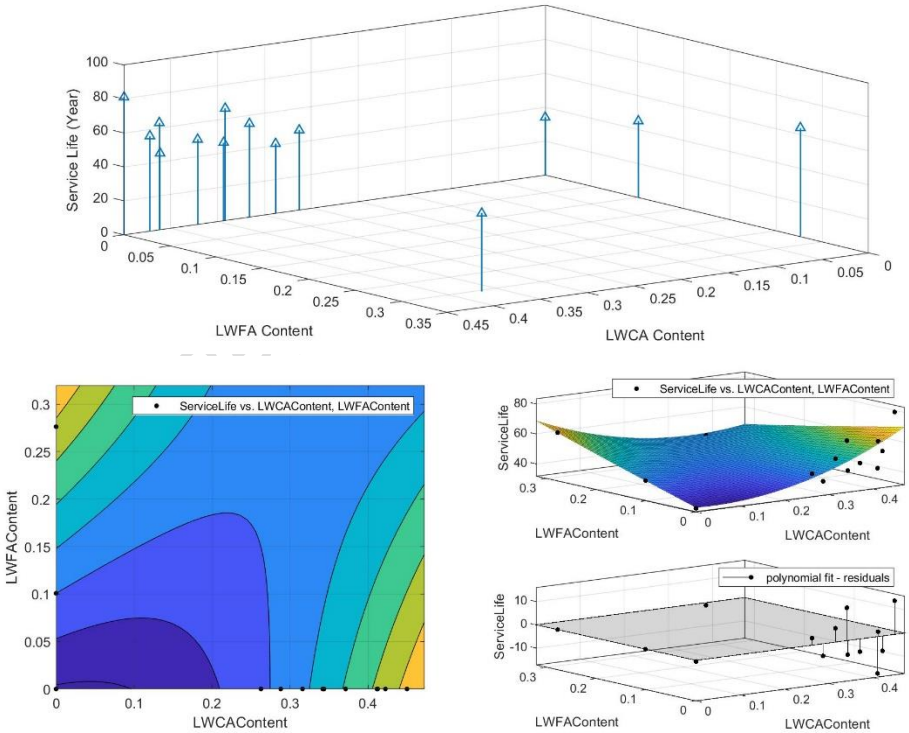

FIGURE 60 TRENDS OF STADIUM® SERVICE LIFE (TOP), FITTING PLANE (MIDDLE), CONTOURS (BOTTOM LEFT), AND ERROR (BOTTOM RIGHT)

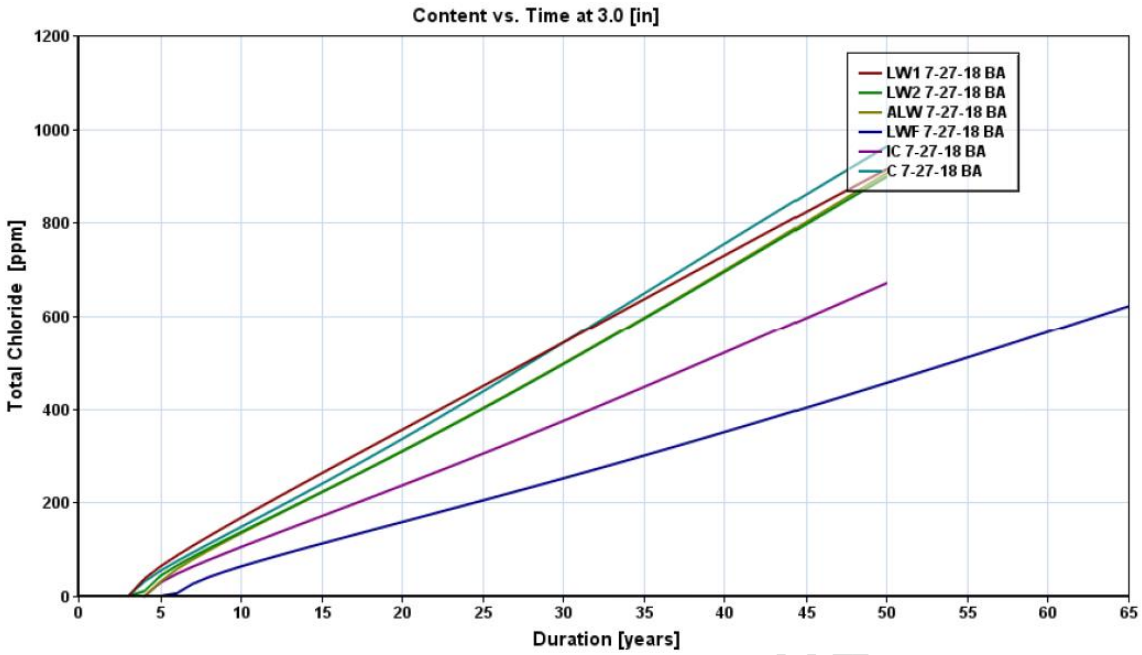

FIGURE 61 STADIUM® CURVES AT 75 MM (3 INCHES) OF COVER FOR A BRIDGE DECK EXPOSURE IN DETROIT, MI

The times to repair for LW1 and LW2 in STADIUM® predictions are higher than the Life 365™ predictions. However, the STADIUM® analysis showed no change in performance for the control, so these LW1 and LW2 mixtures outperform the control mixture by approximately 31% and 75%, respectively. The IC and LWF mixtures had 32% and 88% increase in service life, respectively. Appendix 3 presents the STADIUM® inputs and individual curves.

Figure 62 provides a comparison between two models. As in the Life 365™ analysis, all the LW fine mixtures are significantly outperforming the control mixtures in the STADIUM®, but to a lesser extent than predicted in the Life 365™ modeling. The predicted times to cracking and spalling are equal to or better than the control concrete for all the lightweight mixtures for both analyses.

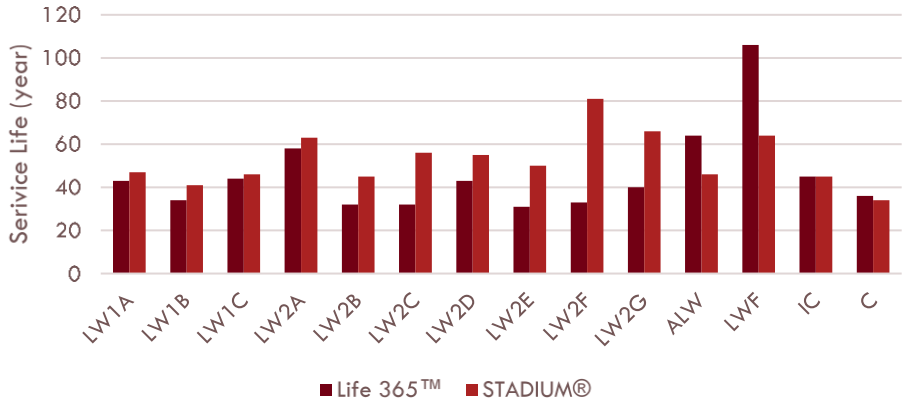

FIGURE 62 PREDICTED SERVICE LIFE OF MIXTURES

3. Conclusions

Transport properties of concretes with LW aggregates were determined versus a control mixture without lightweight aggregate. The service life performance of a bridge deck in the Detroit, MI area was determined using the transport properties applied in the Life 365™ and STADIUM®.

To address the effects of the aggregate porosity, it was necessary to use several test methods and a comparison to a NW aggregate control concrete of the same mixture design and materials.

An internal curing mix with a small quantity of LW fines improved time to restrained shrinkage cracking, produced higher strength, and resulted in a longer service life than the control concrete.

In this study, LW aggregate concrete mixtures were shown to increase the compressive strength of concrete.

Conductivity tests can be used to determine how permeability changes in time, but higher conductivity (corresponding to higher ASTM C1202 rapid chloride permeability), or lower surface resistivity, do not necessarily indicate a higher chloride ingress rate for LW aggregate concrete mixtures. Likewise, the loss of moisture is high in the migration drying tests conducted for STADIUM®. However, the reintroduction of moisture at relative humidity found in regions where deicing salts are used, was found to be reduced using the ASTM C1585 absorption test method.

Results for the control mixture indicated that STADIUM® has underestimated the service life by 3% in comparison to the Life 365™.

The STADIUM® results showed that that the service life would be increased compared to the control as follows:

- For lightweight coarse aggregate mixtures by 21% to 35% in presence of some normalweight course aggregate, and by 32% to 138% without presence of normalweight coarse aggregate. Average values for these series were 31% and 75%, respectively.
- For replacement of normalweight fine with lightweight fine aggregate, the service life increased 32% and 88% for internally cured and reverse lightweight mixtures, respectively.
- The service life of all lightweight aggregate mixture was predicted as 135% of the control mixture.

Life 365™ results analysis showed similar results for LW coarse aggregate mixtures and the normal weight control mixture as follows:

- The increase for lightweight coarse aggregate with and without normalweight coarse aggregate were 33% and 14%, respectively. The later value ranged between 0.86 and 1.64 with a coefficient of deviation of 22% that indicates inconsistencies in modeling.
- The increase in service life for substitution of normalweight fine with lightweight fine aggregate was 25% and 306% for internally cured and reverse lightweight mixtures, respectively.
- The all lightweight aggregate mixture exhibited 64% more service life than the control mixture.
- Comparing data for various climate zones hints that benefits of LWA mixtures for extending the concrete service life are applicable in all zones with maximum benefits in the dry and non-freezing regions as opposed to wet or freezing zones.
- LWA mixtures with FLWA enhance the service life of marine structures within the tidal zone.
- The life cycle cost analyses indicated that application of LWA reduces the life cycle unit cost with negligible 0.001% sensitivity to the cost of LWA aggregate.

Key Finding

The partial substitution of normalweight fine aggregate with lightweight fine aggregate for internal curing reduces restrained shrinkage cracking and increases the compressive strength and the service life. The results for reverse lightweight mixture with normalweight coarse and all lightweight fine aggregates confirms previous result and show even higher predicted service life values. Application of coarse lightweight aggregate also contributes to the enhancement of the compressive strength and the extension of the service life, but outcomes vary depending on the relative contents of lightweight and normalweight aggregates.

Disclaimer

The results and conclusions are based upon the materials tested and the specific mixture design of specimens, the models used, and engineering judgement exercised by the laboratory in charge, Tourney Consulting Group, LLC. Different mixture designs and materials would be expected to follow the trends found, but validation of the transport properties is recommended before modeling. The service life models do not address cracking and the analysis is based on repair of cracks greater than 0.1 mm (0.004 inch) in width.

References

1. Martys, Nicos S. "Survey of concrete transport properties and their measurement." NISTIR 5592, Gaithersburg, MD: National Institute of Standards and Technology (1995).
2. Garboczi, E. J. and D. P. Bentz. "Modeling of the microstructure and transport properties of concrete." *Construction and Building Materials* 10, no. 5 (1996): 293-300.
3. Bentz, Dale P., James R. Clifton, Chiara F. Ferraris, and Edward J. Garboczi. "Transport properties and durability of concrete: literature review and research plan." NISTIR 6395. Gaithersburg, MD: National Institute of Standards and Technology. (1999).
4. Baroghel-Bouny, Veronique, Mickael Thiery, and Xiaomeng Wang. "Performance-based assessment of durability and prediction of RC structure service life: transport properties as input data for physical models." *Materials and Structures* 47 (2014): 1669–1691. https://doi.org/10.1617/s11527-013-0144-z.
5. Zhang, Yong, Mingzhong Zhang. "Transport properties in unsaturated cement-based materials – A review." *Construction and Building Materials* 72 (2014): 367–379. http://dx.doi.org/10.1016/j.conbuildmat.2014.09.037.
6. Weiss, W. J., T. J. Barrett, C. Qiao, and H. Todak. "Toward a Specification for Transport Properties of Concrete Based on the Formation Factor of a Sealed Specimen." *Advances in Civil Engineering Materials* 5, no. 1 (2016): 179-194. doi:10.1520/ACEM20160004.
7. Maltais Y., E. Ouellet, J. Marchand, E. Samson. "14Prediction of the long-term durability of lightweight aggregate concrete mixtures under severe marine environment," in *Advances in Cement and Concrete*, D. A. Lange, K. L. Scrivener and J. Marchand eds. (2003): 329-338. (Proceedings of the ECI conference, Copper Mountain, Colorado, USA, August 10-14, 2003).
8. Thomas, M. D. A. "Chloride Diffusion in High-Performance Lightweight Aggregate Concrete." In *ACI Symposium Paper* 234, 50 (2006): 797-812.
9. Maltais Y., E. Ouellet, J. Marchand, E. Samson, D. Burke. "Prediction of the long-term durability of lightweight aggregate concrete mixtures under severe marine environment." *Materials and Structures* 39 (2006): 911-918.
10. Maltais, Yannick, Eric Ouellet, Jacques Marchand, Eric Samson, Douglas Burke. "Prediction of the long-term durability of lightweight aggregate concrete mixtures under severe marine environment." *Materials and Structures* 39 (2006): 911–918. DOI 10.1617/s11527-006-9127-7.
11. Liu, Xuemei, Kok Seng Chia, Min-Hong Zhang. "Development of lightweight concrete with high resistance to water and chloride-ion penetration." *Cement & Concrete Composites* 32 (2010): 757–766. doi:10.1016/j.cemconcomp.2010.08.005.
12. Ferrer, B., J. A. Bogas, and S. Real. "Service life of structural lightweight aggregate concrete under carbonation-induced corrosion". *Construction and Building Materials* 120, no. 1 (2016): 161–171. https://doi.org/10.1016/j.conbuildmat.2016.05.108.
13. Real, S., J. A. Bogas, and B. Ferrer. "Service life of reinforced structural lightweight aggregate concrete under chloride-induced corrosion." *Materials and Structures* 50, no. 101 (2017). https://doi.org/10.1617/s11527-016-0971-9.
14. Zhen, N., X. Qian, H. Justnes, T. A. Martius-Hammer, K. H. Tan, and K. C. G. Ong. "Durability of lightweight aggregate concrete in marine structures." ISOPE-I-18-649. In *The 28th International Ocean and Polar Engineering Conference*, 10-15 June, Sapporo, Japan: International Society of Offshore and Polar Engineers. 2018.
15. Henkensiefken, Ryan, Javier Castro, Dale Bentz, Tommy Nantung, Jason Weiss. "Water absorption in internally cured mortar made with water-filled lightweight aggregate." Cement and Concrete Research 39 (2009): 883–892. doi:10.1016/j.cemconres.2009.06.009.
16. Schlitter, J., R. Henkensiefken, J. Castro, K. Raoufi, and J. Weiss. "Development of internally cured concrete for increased service life." FHWA/IN/JTRP-2010/10. West Lafayette, IN: INDOT Division of Research. 2010.
17. Castro, Javier, Lucas Keiser, Michael Golias, and Jason Weiss. "Absorption and desorption properties of fine lightweight aggregate for application to internally cured concrete mixtures." *Cement & Concrete Composites* 33 (2011): 1001–1008. doi:10.1016/j.cemconcomp.2011.07.006.
18. Di Bella, Carmelo, Chiara Villani, Elizabeth Hausheer, and William Weiss. "Chloride transport measurements for a plain and internally cured concrete mixture." *ACI Symposium Paper* SP290-14. 2012. DOI: 10.14359/51684183.

19. Zhutovsky, Semion, and Konstantin Kovler. “Effect of internal curing on durability-related properties of high performance concrete.” *Cement and Concrete Research* 42 (2012): 20-26. doi:10.1016/j.cemconres.2011.07.012.
20. Tehrani, F. M. “Deploying and Rating Sustainable Practices for Resilient Bridge Infrastructure.” Keynote Lecture, *Proc. The Fifth International Conference on Bridges*, Amirkabir University of Technology, Tehran. (December 17-18, 2019): MS05. ibc.aut.ac.ir
21. Bonyadian, S., M. Mohammadi, B. Foroutanmehr, and F. M. Tehrani. “An Experimental Investigation of Internally-Cured Concrete Application for Bridge Decks.” *Proc. The Fifth International Conference on Bridges,* Amirkabir University of Technology, Tehran. (December 17-18, 2019): MS02. ibc.aut.ac.ir
22. Bentz, Evan C. “Probabilistic Modeling of Service Life for Structures Subjected to Chlorides.” *ACI Materials Journal* 100, no. 5 (2003): 391-397.
23. Alexander, Mark, and Michael Thomas. “Service life prediction and performance testing - Current developments and practical applications.” *Cement and Concrete Research* 78, Part A (2015): 155-164. https://doi.org/10.1016/j.cemconres.2015.05.013.
24. *fib* Bulleting 34. “Model Code for Service Life Design." Lausanne, Switzerland: fédération internationale du béton, 2006.
25. Papworth, F. and S. Matthews. “*fib* Model Code 2020 - Durability Design and Through Life Management of New and Existing Structures.” In *Proc. Sixth International Conference on Durability of Concrete Structures*, Paper Number KN04, 18 - 20 July 2018, Leeds, West Yorkshire, United Kingdom: University of Leeds (2018): 53-62.
26. Violetta, Brad. “Life-365 Service Life Prediction Model.” *Concrete International* December (2002): 53-57.
27. Ehlen, Mark A., Michael D. A. Thomas, Evan C. Bentz. “Life-365 Service Life Prediction Model™ Version 2.0.” *Concrete International* May (2009): 41-46.
28. Life-365. “Life-365TM service life prediction model TM.” Life-365™ Consortium III, 2013. http://www.life-365.org.
29. Ehlen, Mark A., and Anthony Kojundic. “Life-365™ v2.2.” *Concrete International* May (2014): 41-44.
30. Samson E., J. Marchand, J. J. Beaudoin. “Describing ion diffusion mechanisms in cement-based materials using the homogenisation technique.” *Cement and Concrete Research* 29, no.8 (1999): 1341-1345. https://doi.org/10.1016/S0008-8846(99)00101-5.
31. Samson E., J. Marchand. “Numerical solution of the extended Nernst-Planck model.” *Journal of Colloid and Interface Science* 215 (1999): 1-8.
32. Samson, E., J. Marchand, J. L. Robert, and J. P. Bournazel. “Modelling ion diffusion mechanisms in porous media.” *International Journal for Numerical Methods in Engineering* 46 (1999): 2043-2060.
33. Samson E., J. Marchand, J. J. Beaudoin. “Modeling the influence of chemical reactions on the mechanisms of ionic transport in porous materials: an overview.” *Cement and Concrete Research* 30 (2000): 1895-1902. https://doi.org/10.1016/S0008-8846(00)00458-0.
34. Marchand J., E. Samson, Y. Maltais, J. J. Beaudoin. “Theoretical analysis of the effect of weak sodium sulfate solutions on the durability of concrete.” *Cement and Concrete Composites* 24 (2002): 317-329. https://doi.org/10.1016/S0958-9465(01)00083-X.
35. Samson, E., J. Marchand, K. A. Snyder. “Calculation of ionic diffusion coefficients on the basis of migration test results.” *Materials and Structures* 36 (2003): 156-165. DOI:10.1007/BF02479554.
36. Samson E., J. Marchand, K. A. Snyder, J. J. Beaudoin. “Modeling ion and fluid transport in unsaturated cement systems in isothermal conditions.” *Cement and Concrete Research* 35 (2005): 141-153. doi:10.1016/j.cemconres.2004.07.016.
37. Samson E., J. Marchand. “Modeling the transport of ions in unsaturated cement-based materials.” *Computers and Structures* 85 (2007): 1740-1756. doi:10.1016/j.compstruc.2007.04.008.
38. Henchi K., E. Samson, F. Chapdelaine, J. Marchand. “Advanced finite-element predictive model for the service life prediction of concrete infrastructures in support of asset management and decision-making.” in ASCE Computing in Civil Eng. Conf. Pittsburgh, USA. (2007): 870-880.
39. Samson E., K. Maleki, J. Marchand, T. Zhang. “Determination of the water diffusivity of concrete using drying/absorption test results.” *Journal of the ASTM International 5*, no.7 (2008): Paper ID JAI101322.
40. Marchand J., E. Samson. “Predicting the service-life of concrete structures – Limitations of simplified models.” *Cement & Concrete Composites* 31 (2009): 515-521. https://doi.org/10.1016/j.cemconcomp.2009.01.007.
41. Conciatori D., E. Grégoire, E. Samson, J. Marchand, L. Chouinard. “Statistical analysis of concrete transport properties.” *Materials and Structures* 47 (2014): 89-103.

42. Bu, Y., R. Spragg, C. Villani, and J. Weiss. "The influence of accelerated curing on the properties used in the prediction of chloride ingress in concrete using a Nernst–Planck approach." *Construction and Building Materials* 66 (2014): 752–759. http://dx.doi.org/10.1016/j.conbuildmat.2014.04.138.
43. Weiss, Jason. "Relating transport properties to performance in concrete pavements." MAP Brief December 2014, CP Road Map, Road Map Track 1. 2014.
44. Conciatori D., E. Grégoire E., E. Samson, J. Marchand, L. Chouinard. "Sensitivity of chloride ingress modelling in concrete to input parameter variability." *Materials and Structures* 48 (2015): 3023-3036. DOI 10.1617/s11527-014-0374-8.
45. SIMCO. "Software for transport and degradation in unsaturated materials (STADIUM)." Quebec, Canada: SIMCO Technologies, Inc., 2015.
46. ESCSI. "ESCS Lightweight Aggregate." Chicago, Illinois: Expanded Shale, Clay and Slate Institute (ESCSI). 2015. https://www.escsi.org/escs-lwa/.
47. Lafarge. "Portland Cement." Safety Data Sheet. Chicago: IL: Lafarge. 2019. https://www.lafargeholcim.us/sites/us/files/atoms/files/lafarge_portland_cement_en_190617.pdf.
48. BASF. "MasterAir® 100." Data Sheet. Cleveland, Ohio: BASF Corporation. 2016. https://assets.master-builders-solutions.basf.com/en-tz/basf-masterair-100-tds.pdf.
49. BASF. "MasterGlenium® 7500 Full-Range Water-Reducing Admixture." Data Sheet. Cleveland, Ohio: BASF Corporation. 2018. https://assets.master-builders-solutions.basf.com/en-us/basf-masterglenium-7500-tds.pdf.
50. ASTM C143 / C143M-15a. "Standard Test Method for Slump of Hydraulic-Cement Concrete." West Conshohocken, PA: ASTM International. 2015. 10.1520/C0143_C0143M-15A.
51. ASTM C231 / C231M-17a. "Standard Test Method for Air Content of Freshly Mixed Concrete by the Pressure Method." West Conshohocken, PA: ASTM International. 2017. 10.1520/C0231_C0231M-17A.
52. ASTM C457 / C457M-16. "Standard Test Method for Microscopical Determination of Parameters of the Air-Void System in Hardened Concrete." West Conshohocken, PA: ASTM International. 2016. 10.1520/C0457_C0457M-16.
53. ASTM C403 / C403M-16. "Standard Test Method for Time of Setting of Concrete Mixtures by Penetration Resistance." West Conshohocken, PA: ASTM International. 2016. 10.1520/C0403_C0403M-16.
54. ASTM C1064 / C1064M-17. "Standard Test Method for Temperature of Freshly Mixed Hydraulic-Cement Concrete." West Conshohocken, PA: ASTM International. 2017. 10.1520/C1064_C1064M-17.
55. ASTM C39 / C39M-16. "Standard Test Method for Compressive Strength of Cylindrical Concrete Specimens." West Conshohocken, PA: ASTM International. 2016. 10.1520/C0039_C0039M-16.
56. ASTM C566-13. "Standard Test Method for Total Evaporable Moisture Content of Aggregate by Drying." West Conshohocken, PA: ASTM International. 2013. 10.1520/C0566-13.
57. ASTM C192 / C192M-16a. "Standard Practice for Making and Curing Concrete Test Specimens in the Laboratory." West Conshohocken, PA: ASTM International. 2016. 10.1520/C0192_C0192M-16A.
58. ASTM C511-13. "Standard Specification for Mixing Rooms, Moist Cabinets, Moist Rooms, and Water Storage Tanks Used in the Testing of Hydraulic Cements and Concretes." West Conshohocken, PA: ASTM International. 2013. 10.1520/C0511-13.
59. ACI Committee 211. "Standard Practice for Selecting Proportions for Normal, Heavyweight, and Mass Concrete." ACI 211.1-91 (Reapproved 2009). Farmington Hills, MI: American Concrete Institute. 2002.
60. ASTM C1761 / C1761M-17. "Standard Specification for Lightweight Aggregate for Internal Curing of Concrete." West Conshohocken, PA: ASTM International. 2017. 10.1520/C1761_C1761M-17.
61. ASTM C1760-12. "Standard Test Method for Bulk Electrical Conductivity of Hardened Concrete." West Conshohocken, PA: ASTM International. 2012. 10.1520/C1760-12.
62. ASTM C1202-17. "Standard Test Method for Electrical Indication of Concrete's Ability to Resist Chloride Ion Penetration." West Conshohocken, PA: ASTM International. 2017. 10.1520/C1202-17.
63. NT BUILD 492. "Concrete, mortar and cement-based repair materials: Chloride migration coefficient from non-steady state migration experiments." Espoo, Finland: Nordtest. 1999.
64. ASTM C1556-11a. "Standard Test Method for Determining the Apparent Chloride Diffusion Coefficient of Cementitious Mixtures by Bulk Diffusion." West Conshohocken, PA: ASTM International. 2016. 10.1520/C1556-11AR16.
65. ASTM C1585-13. "Standard Test Method for Measurement of Rate of Absorption of Water by Hydraulic-Cement Concretes." West Conshohocken, PA: ASTM International. 2013. 10.1520/C1585-13.

66. ASTM C1581 / C1581M-18a. "Standard Test Method for Determining Age at Cracking and Induced Tensile Stress Characteristics of Mortar and Concrete under Restrained Shrinkage." West Conshohocken, PA: ASTM International. 2018. 10.1520/C1581_C1581M-18A.
67. ASTM C642-13. "Standard Test Method for Density, Absorption, and Voids in Hardened Concrete." ASTM International, West Conshohocken, PA: ASTM International. 2013. 10.1520/C0642-13.
68. NYDOT. "Moisture Content of Lightweight Fine Aggregate." Test Method NY 703-19 E. Albany, NY: New York Department of Transportation. 2008. 10.1520/C1581_C1581M-18A. https://www.dot.ny.gov/divisions/engineering/technical-services/materials-bureau-repository/tm_703-19E.pdf.
69. ASTM C567 / C567M-14. "Standard Test Method for Determining Density of Structural Lightweight Concrete." ASTM International, West Conshohocken, PA: ASTM International. 2014. 10.1520/C0567_C0567M-14.
70. Weiss, Jason, Ken Snyder, Jeff Bullard, and Dale Bentz. "Using a Saturation Function to Interpret the Electrical Properties of Partially Saturated Concrete." *Journal of Materials in Civil Engineering* 25, no. 8 (2013): 1097-1106. DOI: 10.1061/(ASCE)MT.1943-5533.0000549.
71. Bu, Yiwen, Daming Luo, and Jason Weiss. "Using Fick's Second Law and Nernst-Planck Approach in Prediction of Chloride Ingress in Concrete Materials." *Advances in Civil Engineering Materials* 3, no.1 (2014): 566-584. doi:10.1520/ACEM20140018.
72. Bu, Y., R. Spragg, W. J. Weiss. "Comparison of the Pore Volume in Concrete as Determined Using ASTM C642 and Vacuum Saturation." *Advances in Civil Engineering Materials* 3, no. 1 (2014): 308-315. DOI: 10.1520/ACEM20130090.
73. Bu, Yiwen, and Jason Weiss. "The influence of alkali content on the electrical resistivity and transport properties of cementitious materials." *Cement & Concrete Composites* 51 (2014): 49–58. http://dx.doi.org/10.1016/j.cemconcomp.2014.02.008.
74. De la Varga, Igor, Robert P. Spragg, Carmelo Di Bella, Javier Castro, Dale P. Bentz, and Jason Weiss. "Fluid transport in high volume fly ash mixtures with and without internal curing." *Cement & Concrete Composites* 45 (2014): 102–110. http://dx.doi.org/10.1016/j.cemconcomp.2013.09.017.
75. Spragg, R. P., C. Villani, J. Weiss, A. Poursaee, S. Jones, D. P. Bentz, and K. A. Snyder. "Surface and Uniaxial Electrical Measurements on Layered Cementitious Composites having Cylindrical and Prismatic Geometries." *Proc. 4th International Conference on the Durability of Concrete Structures* (24–26 July 2014). West Lafayette, IN: Purdue University. (2014): 317-326.
76. ESCSI. "Guide for Calculating the Quantity of Prewetted ESCS Lightweight Aggregates for Internal Curing." Internal Curing Calculator. Chicago, IL: Expanded Shale, Clay and Slate Institute. 2018. https://www.escsi.org/internal-curing/ic-calculator/.
77. Thomas, Michael D.A., and Phil B. Bamforth. "Modelling chloride diffusion in concrete: Effect of fly ash and slag." *Cement and Concrete Research* 29, no. 4 (1999): 487-495. https://doi.org/10.1016/S0008-8846(98)00192-6.
78. Audenaert, K., Q. Yuan, G. De Schutter. "On the time dependency of the chloride migration coefficient in concrete." *Construction and Building Materials* 24 (2010): 396–402.
79. Boddy, Andrea, Evan Bentz, M. D. A. Thomas, R. D. Hooton. "An overview and sensitivity study of a multimechanistic chloride transport model." *Cement and Concrete Research* 29 (1999): 827–837.
80. Andrade, C., M. Castellote, R. d'Andrea. "Measurement of ageing effect on chloride diffusion coefficients in cementitious matrices." *Journal of Nuclear Materials* 412, no. 1 (2011): 209-216. https://doi.org/10.1016/j.jnucmat.2010.12.236.
81. Schwartz, C. W., G. E. Elkins, R. Li, B. A. Visintine, B. Forman, G. R. Rada, and J. L. Groeger. "Evaluation of long-term pavement performance (LTPP) climate data for use in mechanistic-empirical pavement design guide (MEPDG) calibration and other pavement analysis." FHWA-HRT-15-019. Washington, DC: Federal Highway Administration. 2015. https://www.fhwa.dot.gov/publications/research/infrastructure/pavements/ltpp/15019/010.cfm.
82. Vosoughi, P. S. Tritsch, H. Ceylan, and P. Taylor. "Lifecycle Cost Analysis of Internally Cured Jointed Plain Concrete Pavement." Part of IHRB Project TR-676. Ames, IA: National Concrete Pavement Technology Center. 2017.